

**POLITECNICO DI TORINO**

**Master's Degree in Energy and Nuclear Engineering**



**Politecnico  
di Torino**

**Master's Degree Thesis**

**Hydrogen deblending on the gas  
transmission network and gas quality  
assessment: Sicily case study**

**Supervisors**

**Prof. Pierluigi LEONE**

**PhD Marco CAVANA**

**Candidate**

**Madalina Luiza CHIRICHES**

**November 2023**



# Summary

This master's thesis presents a comprehensive study on the deblending of hydrogen within the natural gas transmission network, with a specific focus on the Southern Sicily region.

The research investigates the behavior of a gas mixture originating from North Africa, composed of natural gas and green hydrogen in different concentrations, considering a 5%, 10%, and 20% blend. The gas network was modeled using data from the National Transmission System Operator and GIS tools, with topology analysis performed with MATLAB for simulation purposes.

The simulations include an examination of the gas mixture's behavior throughout the pipelines, emphasizing the deblending process at the network's final nodes, corresponding to delivery points. Separated hydrogen is then progressively reinjected into the network, gradually increasing its concentration as it progresses. The final target is an industrial area with multiple refineries, where a higher hydrogen concentration is desired. For each blending scenario, an analysis is conducted to assess the hydrogen accumulation and the quality of the gas, including considerations of relative density, Wobbe Index, and Higher Heating Value, ensuring compliance with relevant standards.

This research has the aim of contributing to our understanding of the integration of hydrogen into existing natural gas infrastructure and its potential for enhancing the sustainability of energy transportation networks.

# Acknowledgements

The first expression of gratitude is dedicated to my family, who has consistently granted me the freedom to choose my own path and has emphatically supported me in my decisions. I extend my heartfelt thanks to my parents, who, despite being physically distant, have always wanted to provide support in every possible way, making significant sacrifices. I express my gratitude to my brother, Silviu, who has been a friend, advisor, and both moral and physical support in recent years.

Special thanks go to my boyfriend, Giacomo, for being by my side during the moments of joy, but most importantly, during the challenging ones. I cannot imagine reaching the end of this journey without your unwavering support, the example you've set, and the strength you've managed to impart to me.

I would like to thank Elena, my best friend since friends are chosen by will, not by chance. Despite difficulties, distances, and diverging paths, you have been like a sister to me.

Much appreciation go to Davide and Cecilia, invaluable friends and study companions. Over the past four years, you have lightened the academic load, and I appreciate the motivation and support you've consistently provided.

Special thanks go to Roberto and Marcello, classmates for a short time, but friends I hope for much longer.

I would like to express my gratitude to my supervisors, professor Leone and Marco. For giving me the opportunity to work on a topic that proved to be of great interest for me, for allowing me to forward into a first valuable work experience, and for supporting me since the early stages of this work.

Finally, I would like to thank everyone who became a part of my life during this journey. Those who left, those who have only been passing through, those who recently arrived and whose presence is currently indefinite. I thank you, because it is also by getting to know you, drawing inspiration from your qualities, and learning from your mistakes that I have become the person I am today.

*Thank you,  
Madalina*



# Table of Contents

<b>List of Tables</b>	VII
<b>List of Figures</b>	VIII
<b>1 Introduction</b>	1
1.1 A European overview . . . . .	2
1.1.1 The European Green Deal . . . . .	2
1.1.2 A Hydrogen strategy for a climate-neutral Europe . . . . .	4
1.2 Hydrogen as a green energy carrier . . . . .	6
1.2.1 Hydrogen production technologies . . . . .	7
1.2.2 Present and future hydrogen applications . . . . .	8
1.2.3 Global hydrogen resources and demand . . . . .	10
1.3 Hydrogen transport and handling . . . . .	12
1.4 Scope and structure of the study . . . . .	14
<b>2 Hydrogen integration in the existing gas infrastructure</b>	15
2.1 The European Hydrogen Backbone . . . . .	16
2.1.1 Transmission System Operators . . . . .	19
2.2 Hydrogen users and integration limitations . . . . .	21
2.3 Hydrogen and natural gas blending . . . . .	24
2.4 Hydrogen debblending . . . . .	28
2.4.1 Pressure Swing Adsorption . . . . .	29
2.4.2 Polymeric membrane separation . . . . .	31
2.4.3 Cryogenic separation . . . . .	32
<b>3 Methodology</b>	34
3.1 Case study selection . . . . .	34
3.2 Network modelling and data preparation . . . . .	37
3.2.1 Network modeling through QGIS . . . . .	38
3.2.2 Data preparation . . . . .	43
3.3 SIMPLE algorithm and debblending model . . . . .	45

3.3.1	Pressure Drop and Mass Equations . . . . .	45
3.3.2	<i>SIMPLE</i> Algorithm . . . . .	49
3.4	Deblending model . . . . .	52
<b>4</b>	<b>Simulations and results</b>	<b>55</b>
4.1	Simulation settings . . . . .	55
4.2	Base case: no hydrogen blending . . . . .	57
4.3	5% Hydrogen blending . . . . .	59
4.4	10% Hydrogen blending . . . . .	63
4.5	20% Hydrogen blending . . . . .	65
<b>5</b>	<b>Discussion of results and conclusions</b>	<b>67</b>
5.1	Discussion of results . . . . .	67
5.2	Future developments . . . . .	74
5.3	Conclusions . . . . .	75
	<b>Bibliography</b>	<b>76</b>

# List of Tables

2.1	Property comparison of hydrogen and methane [37] . . . . .	25
3.1	Nodes' Coordinates X and Y . . . . .	40
3.2	Branches data . . . . .	41
3.3	Entry points and mass flow . . . . .	43
3.4	Delivery points capacity and pressure . . . . .	44
4.1	Recovery Rate and Purity for each final user typology . . . . .	55
4.2	Mass flow rate of extracted hydrogen - 5% blend case . . . . .	62
4.3	Mass flow rate of extracted hydrogen - 10% blend case . . . . .	64
4.4	Mass flow rate of extracted hydrogen - 20% blend case . . . . .	66
5.1	Allowable ranges of the $HHV$ , $WI$ and $\rho$ in Italy [52] . . . . .	68
5.2	Air, Hydrogen and natural gas densities in standard conditions . . .	68
5.3	Hydrogen and natural gas higher heating values in standard conditions	68
5.4	Gas quality variations with % $H_2$ . . . . .	69
5.5	Hydrogen share acceptability limit . . . . .	71
5.6	Hydrogen flow on focus pipeline . . . . .	72
5.7	Total $H_2$ extraction in the three scenarios . . . . .	73

# List of Figures

1.1	The European Green Deal targets [3] . . . . .	3
1.2	Hydrogen’s potential for Europe [6] . . . . .	4
1.3	Worldwide hydrogen production and consumption, 2018 [15] . . . . .	9
1.4	Global hydrogen resources and demand centers [16] . . . . .	11
2.1	Companies participating in the EHB initiative [22] . . . . .	16
2.2	Accelerated 2030 EHB network with its cross-border corridors [22] .	18
2.3	Main hydrogen separation technologies [41] . . . . .	29
2.4	Typical Pressure Swing Adsorbtion cycle [41] . . . . .	30
2.5	Typical Membrane separation flowsheet [41] . . . . .	31
2.6	Typical Cryogenic separation flowsheet [41] . . . . .	32
3.1	National Transmission System in Italy [26] . . . . .	35
3.2	Syracuse petrochemical hub [44] . . . . .	36
3.3	Sicilian Transmission Network representation [45] . . . . .	38
3.4	Sicilian reduced Transmission Network model representation . . . . .	39
3.5	Sicilian reduced Transmission Network model check on MATLAB .	42
3.6	Sicilian reduced Transmission Network model on MATLAB, cosider- ing coordinates . . . . .	42
3.7	Schematized portion of a generic pipe . . . . .	45
3.8	Moody Diagram [51] . . . . .	48
3.9	Scheme of the deblanding unit represented as a black box . . . . .	52
4.1	Network model on MATLAB, considering coordinates . . . . .	56
4.2	Nodal pressures and flow rates . . . . .	57
4.3	Gas flow rates at network boundaries . . . . .	58
4.4	Pipeline flow rates . . . . .	58
4.5	Hydrogen distribution through the network without $H_2$ extraction - 5% blend case . . . . .	59
4.6	Hydrogen distribution through the network with $H_2$ extraction - 5% blend case . . . . .	60

4.7	Comparison of hydrogen extraction area - with and without $H_2$ extraction . . . . .	60
4.8	$H_2$ share distribution without extraction - 5% blend case . . . . .	61
4.9	$H_2$ share distribution with extraction - 5% blend case . . . . .	61
4.10	Hydrogen distribution through the network with extraction - 10% blend case . . . . .	63
4.11	$H_2$ share distribution with extraction - 10% blend case . . . . .	64
4.12	Hydrogen distribution through the network with extraction - 20% blend case . . . . .	65
4.13	$H_2$ share distribution with extraction - 20% blend case . . . . .	66
5.1	Higher Heating Value trend based on percentage of $H_2$ in the mixture	69
5.2	Wobbe Index trend based on percentage of $H_2$ in the mixture . . . . .	70
5.3	Relative density trend based on percentage of $H_2$ in the mixture . . . . .	70
5.4	Geographic location of the high demand node in the area . . . . .	72



# Chapter 1

## Introduction

The current energy transition has identified electrification as one of the key factors in achieving carbon neutrality. Unfortunately, a high degree of electrification brings with it costs, supply security and resilience concerns that need to be thoroughly investigated and resolved before widespread adoption. Recent exponential deployment and cost reductions have made solar and wind energy a cost-effective source of renewable energy, especially in the most favorable areas. However, limitations arise in storing such energy, in the transportation sector, and in meeting the demands of industrial processes that require high-temperature heat and chemical feedstock. Different geographical and demographic characteristics, along with the fact that the most sites for the production of renewable energy are generally located far from high-consumption areas, underlines the need to import and/or exchange a significant part of renewable energy over long distances.

Therefore, it is important to involve all sectors of our economy in order to drastically reduce carbon emissions. Hydrogen, by addressing some of the aforementioned problems, is considered to play a crucial role in 2050 climate neutrality targets. The European Green Deal (EGD) has set the course for the EU to become the world's first carbon neutral continent by 2050 [1].

## 1.1 A European overview

### 1.1.1 The European Green Deal

On December 2019 the European Commission unveiled the European Green Deal to both the public and the EU institutions. Following a parliamentary debate in January 2020, the European Parliament expressed its support for the Green Deal but underscored the need for additional efforts to ensure an equitable transition and called for more ambitious interim targets, particularly in the context of carbon emissions.

The Green Deal is not a legal framework in itself but rather a broad policy strategy outlining ambitions and objectives in several policy domains. To put it into action, existing regulations and standards need to be reviewed, and new laws and directives have been crafted and put into effect [2]. This strategy has a primary objective of reshaping the European Union into an equitable and thriving society. It envisions a modern, resource-efficient, and competitive economy that achieves a state of no net emissions of GHG by the year 2050 along with seeking the separation of economic growth from the utilization of resources [3].

On June 24, 2021, the European Parliament passed the EU Climate Law, a significant legislative milestone that enforces a binding commitment to reduce emissions by 55% by the year 2030 and achieve climate neutrality by 2050 [4].

The Green Deal consists of eight key targets:

1. Elevating the European Union's climate aspirations for both 2030 and 2050.
2. Ensuring the provision of clean, cost-effective, and secure energy.
3. Galvanizing the industrial sector to promote a clean and circular economy.
4. Promoting energy and resource-efficient construction and renovation practices.
5. Aspiring to achieve zero pollution with the goal of creating a toxic-free environment.
6. Safeguarding and restoring ecosystems and biodiversity.
7. Advancing the Farm to Fork initiative, which aims to establish a just, healthy, and environmentally friendly food system.
8. Speeding up the transition to sustainable and smart mobility solutions [2].

The key targets of the European Green Deal are shown in figure 1.1

The primary objective of the first five pathways is to gain a deeper understanding of the available options for emission reduction and how these options will influence the



**Figure 1.1:** The European Green Deal targets [3]

transformations within the sectors of our economy. The main focus is on achieving emissions reduction of over 80% by 2050 compared to 1990 levels.

The sixth pathway combines the cost-effective opportunities for greenhouse gas (GHG) reduction from the first five pathways, resulting in the perspective of achieving GHG reductions of up to 90%.

The seventh and eighth pathways are dedicated to evaluating the means by which net-zero greenhouse gas emissions, or climate-neutrality, can be attained by 2050, and to examining the role of net negative emissions in the process of achieving zero greenhouse gas emissions by 2050.

More particularly, the seventh target focuses on adopting zero-carbon energy carriers while depending on  $CO_2$  removal technologies through combining bioenergy and Carbon Capture and Storage (CCS) to counterbalance emissions. The eighth pathway, on the other hand, offers more aptitude to enhance the land use sink and requires fewer dependencies on  $CO_2$  removal technologies to offset any remaining emissions. It places a greater emphasis on the influence of a circular economy, particularly in a scenario where consumer choices become less carbon-intensive [5].

### 1.1.2 A Hydrogen strategy for a climate-neutral Europe

Thanks to recent developments, including the declining costs of renewable energy and the urgency of reducing greenhouse emissions, hydrogen has become a focal point in achieving the European Green Deal and Europe’s transition to clean energy. Although renewable electricity is expected to decarbonize a significant portion of EU energy consumption by 2050, hydrogen can play a significant role by serving as a vector for renewable energy storage and transportation, offering backup for seasonal variations and connecting production sites to distant demand centers. The strategic vision for a climate-neutral EU aims to increase the share of hydrogen in Europe’s energy mix from less than 2% [6] to more than 23% by 2050 [7], as seen in figure 1.2.

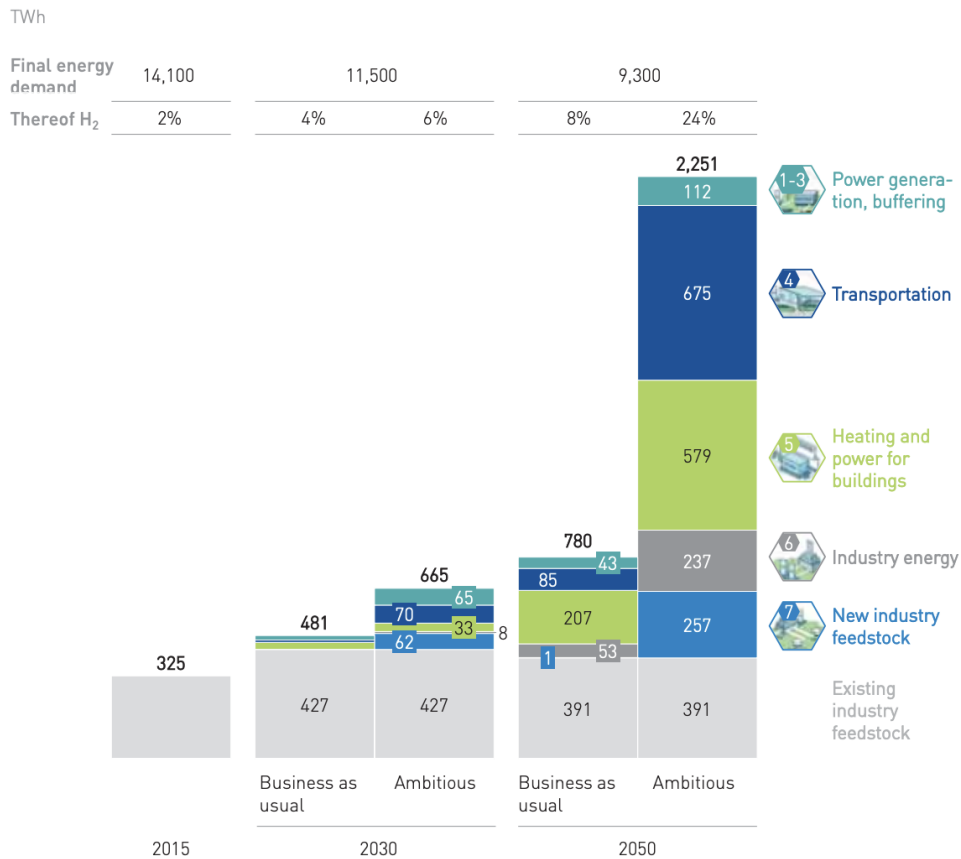


Figure 1.2: Hydrogen’s potential for Europe [6]

In the integrated energy system of the future, hydrogen will play a vital role alongside renewable electrification and a more efficient, circular use of resources.

Swift and large-scale deployment of clean hydrogen is essential for the EU to achieve higher climate ambitions, including reducing greenhouse gas emissions by a minimum of 50% and moving towards 55% by 2030, all in a cost-effective manner. Moreover hydrogen, by reducing GHG emissions, has the potential to replace fossil fuels in carbon-intensive industrial processes, such as steel and chemical manufacturing, thus to enhance the global competitiveness of these industries. It can also address challenging aspects of the transportation system that cannot be easily electrified or serviced by other renewable or low-carbon fuels . Investing in hydrogen will promote sustainable growth and job creation, which is especially critical as part of the recovery from the COVID-19 crisis. The Commission’s recovery plan underscores the importance of unlocking investment in key clean technologies and value chains and highlights clean hydrogen as a crucial area to address in the context of the energy transition, offering several possible avenues for support and development [8].

In line with the European Green Deal [3] and building upon the Commission’s *New Industrial Strategy* [9] and Recovery Plan [8], the *Hydrogen strategy for a climate-neutral Europe* outlines a vision for making clean hydrogen a practical solution for decarbonizing various sectors. It sets the target of installing at least 6 GW of renewable hydrogen electrolyzers in the EU by 2024 and 40 GW by 2030 [10]. Given the long investment cycles in the clean energy sector, immediate action is necessary. This strategic roadmap provides a concrete policy framework, and the newly launched European Clean Hydrogen Alliance will develop an investment agenda and projects. It complements the *Strategy for Energy System Integration*, promoting a climate-neutral integrated energy system with a focus on renewable electricity, circularity, and renewable and low-carbon fuels [11].

Deploying hydrogen in Europe presents significant challenges that require a collective effort and its development needs substantial investment, a supportive regulatory framework, new markets, continuous research, and a vast infrastructure network. Collaboration between public and private entities at various levels is essential to establish a vibrant hydrogen ecosystem in Europe.

## 1.2 Hydrogen as a green energy carrier

Hydrogen serves as a carbon-free energy carrier and will play a pivotal role in the future sustainable energy system. It is an efficient alternative for transportation and storage of renewable energy from resource-rich remote areas to where it's needed, matching supply with demand.

It is a versatile element that can serve as a feedstock, a fuel, or an energy carrier and storage medium, offering a wide range of potential applications in various sectors such as industry, transportation, power generation, and buildings. Additionally, hydrogen combustion produces minimal  $CO_2$  emissions and almost no air pollution, making it a valuable solution for decarbonizing industries and sectors where carbon emission reduction is a pressing and challenging goal. For these reasons, hydrogen is currently experiencing a rapid growth in attention both in Europe and globally [10].

Despite its potential, hydrogen currently represents only a small fraction of the global and European energy mix, and it is primarily produced from fossil fuels which leads to the emission of 70 to 100 million tonnes of  $CO_2$  annually in the EU. To make hydrogen a contributor to climate neutrality, its production must transition to being fully decarbonized [6].

In addition to its systemic role, hydrogen is crucial for decarbonizing challenging sectors such as industry, transportation, electricity grid balancing, and heating. Nevertheless, in time, cost competition will likely emerge between imported renewable hydrogen and locally produced renewable hydrogen and electricity.

A dedicated H<sub>2</sub> infrastructure can be developed by repurposing existing gas infrastructure, including pipelines and salt cavern storage facilities, also at global level. Future hydrogen systems are expected to resemble present-day natural gas systems.

During an interim phase, natural gas can be converted into hydrogen at the source without emitting  $CO_2$ , resulting in no-carbon fossil hydrogen. This allows for a rapid transition to hydrogen as an energy carrier and commodity. As time progresses, an increasing share of hydrogen from solar and wind sources can be integrated into the system, eventually replacing no-carbon fossil hydrogen entirely. This comprehensive system approach offers a fast, cost-effective, reliable, secure, and inclusive path to a sustainable energy system [12]. As mentioned in section 1.1.2, on July 8, 2020, the European Commission unveiled the EU Hydrogen Strategy within the framework of the European Green Deal. This strategy sets out ambitious targets, including the production of 1 million tonnes of clean hydrogen per year and the establishment of an electrolyser capacity of 6GW by 2024, with the aim of reaching 10 million tonnes per year and at least 40GW of electrolyser capacity by 2030. Additionally, the strategy underscores the importance of hydrogen import from neighboring regions, particularly North Africa [10].

The primary objectives of the current hydrogen strategies include [13]:

- Reducing greenhouse gas emissions, with a particular focus on challenging sectors.
- Diversifying the energy supply to enhance energy security and resilience.
- Integrating renewable energy sources into the energy mix.
- Fostering economic growth through the development of a hydrogen industry.
- Supporting national technology advancements and innovation.
- Ensuring security of supply and strategic reserves.
- Exploring opportunities for hydrogen export and import, contributing to global trade and energy security.

### 1.2.1 Hydrogen production technologies

As a carbon-free energy carrier, when burned or converted hydrogen does not release  $CO_2$  emissions into the atmosphere. However, when considering the entire life cycle of hydrogen, its production may involve certain  $CO_2$  emissions, whose extents depend on the source of hydrogen and the technology used for the conversion.

The main sources for hydrogen production are:

1. Fossil Fuels: the energy input comes from hydrogen-carbon molecules. This process generates  $CO_2$  emissions.
2. Biomass Resources: where the energy comes from the biomass itself, meaning hydrogen-oxygen-carbon molecules. This process may involve  $CO_2$  emissions, depending on the source and processing methods.
3. Water: when water is used as the source of hydrogen, the energy input can come from different methods [12]:
  - Electricity: through electrolysis, which involves splitting water into hydrogen and oxygen using electricity.
  - Heat: Using thermolysis, where heat is applied to split water into its constituent elements.
  - Solar Light-Photons: using photolysis or photo-electrochemical processes, where sunlight directly splits water into hydrogen and oxygen.

The key to determining whether direct or indirect CO<sub>2</sub> emissions occur lies in the combination of the energy source, the conversion process, the input energy, and the flue gas treatment processes. These factors collectively define the 'color' associated with hydrogen production, as summarized in the following table.

Hydrogen production from fossil fuels, such as natural gas, could potentially have zero CO<sub>2</sub> emissions. Presently, Steam Methane Reforming (SMR) plants are used for hydrogen production from natural gas, resulting in CO<sub>2</sub> emissions. In the future, Auto Thermal Reforming (ATR) plants, which produce two distinct CO<sub>2</sub> flows, may be employed. It is possible to capture up to 100% of the pure CO<sub>2</sub> flow from ATR processes. However, capturing CO<sub>2</sub> from the flue gas, which contains CO<sub>2</sub> from burning natural gas for heat, is more challenging and costly. Therefore, it is believed that up to 90% of the CO<sub>2</sub> can be captured and stored at ATR plants.

A technology in development is the photo-electrochemical cell, which has the potential to use sunlight to split water molecules into hydrogen and oxygen without the need for separate electrolysis. This innovation is currently undergoing research to optimize efficiency, reduce material usage, minimize degradation, and achieve a stable process. Repsol, a Spanish oil company, has even announced the commercial viability of 'direct solar-to-hydrogen' without the intermediary of electrolysis by 2030.

Finally, methane pyrolysis can split methane (CH<sub>4</sub>) into hydrogen (H<sub>2</sub>) and solid carbon (C) without generating any CO<sub>2</sub>. The presence or absence of indirect CO<sub>2</sub> emissions depends on the energy source used for the process. If renewable or nuclear resources are employed to produce hydrogen and electricity, the process can be entirely free of CO<sub>2</sub> emissions [14].

### 1.2.2 Present and future hydrogen applications

Hydrogen, in its pure form, is not widely used as an energy carrier in the public domain, especially for heating buildings and transportation. Additionally, hydrogen is underrepresented or only beginning to gain consideration within energy laws and regulations.

Currently, hydrogen is mostly used as feedstock for the production of chemical products, including ammonia and methanol and its production is primarily sourced from natural gas and coal. The energy required for hydrogen production from these two sources accounts for approximately 3,200 terawatt-hours (TWh), constituting around 2% of global primary energy consumption, as illustrated in figure 1.3.

Hydrogen also plays an important role in oil refineries for desulfurizing oil and in the manufacturing of kerosene, gasoline, and diesel. Therefore, at the moment the majority of hydrogen production occurs in close proximity to chemical and petrochemical facilities. In these cases, natural gas is transported via pipelines,

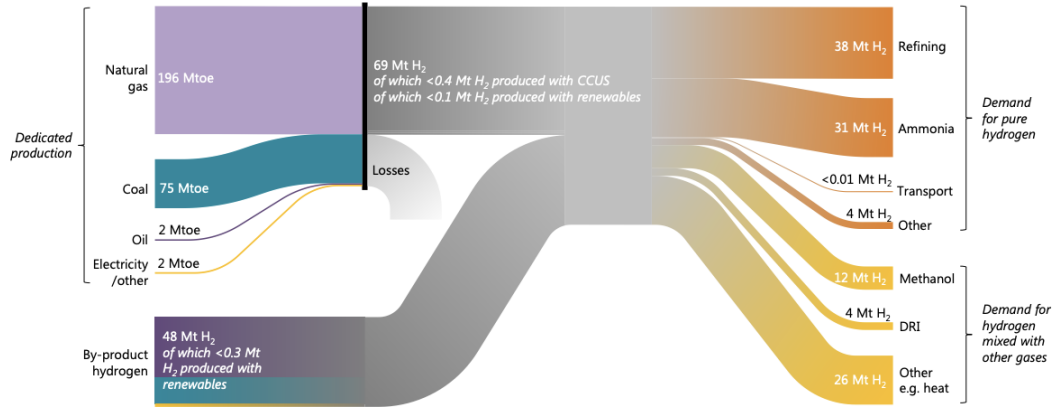


**Figure 1.3:** Worldwide hydrogen production and consumption, 2018 [15]

while coal is shipped by sea, rail, or road to refineries, fertilizer, or methanol plants, where they are converted into hydrogen. This on-site production and usage of hydrogen is referred to as "captive hydrogen production and use". There is a limited private-owned hydrogen pipeline infrastructure at chemical sites, primarily to ensure a reliable baseload supply [12].

During a transitional period, hydrogen can be utilized through combustion in boilers, furnaces, engines, or turbines to generate heat, electricity, or mechanical power. Nevertheless in the future, electrochemical conversion using fuel cells will gain greater significance as they have been developed significantly in recent years, particularly by car manufacturers for mobility applications in electric vehicles. Fuel cells share a similar technology structure with electrolyzers, batteries, and solar systems, consisting of cells stacked together to form a fuel cell system. However, Research and development are critical for cost reduction, increased efficiency, reduced degradation, and the reduction of materials, particularly platinum. Fuel cell Capex costs are anticipated to be lower, with higher conversion efficiencies compared to conventional combustion technologies, such as engines or turbines. Thus, fuel cell technology is expected to become at least cost-competitive, and in most cases, cheaper than current combustion technology in the future.

The fuel cell mobility systems abovementioned have broader applications in various modes of transportation, including ships, trains, drones, and planes. Additionally, fuel cell systems will play a crucial role in other applications, as they can be used in homes and buildings to produce electricity and heat as the volume and temperature of the generated heat can be adjusted to meet specific requirements using heat pumps. In addition to providing heat, the electricity generated by fuel cells complements the power from solar panels on rooftops. Fuel cell systems can also serve as electricity balancing plants, and can be distributed in decentralized

locations, such as villages, neighborhoods, and office sites, to produce electricity and heat locally, enhancing energy resilience and sustainability [12].

### 1.2.3 Global hydrogen resources and demand

While many regions worldwide can produce low-cost renewable hydrogen, it's clear that some will become net exporters while others become net importers. Even within regions, there will be a trade in hydrogen. Low-cost green hydrogen production is feasible where there are extensive solar and/or wind resources, but large-scale production will be limited.

More specifically, Japan, South Korea, parts of China, parts of the USA, the European Union, and India will likely become net importers of low-cost hydrogen due to their limited renewable resources, restricted land area, and high population density. A study using GIS and data has identified the Sahara Desert as the most cost-effective location for both solar and land-based wind hydrogen production in Europe and North Africa. Offshore wind also presents potential for low-cost production.

North Africa has significant hydrogen production potential, exceeding six times the world's primary energy consumption. In contrast, Northwest and Mid-European countries have limited potential for low-cost renewable hydrogen due to resource and land constraints, making them net importers.

However, hydrogen production should be situated near energy resources and connected to a hydrogen infrastructure. High-quality solar and wind resources are unevenly distributed globally, often far from energy demand centers as shown in figure 1.4. In regions where renewable electricity production is constrained by factors like land availability, population density, or environmental restrictions, large-scale hydrogen conversion becomes essential.

Multi-GW production of solar and wind electricity in resource-rich locations, conversion to hydrogen, and transportation can provide abundant, affordable renewable electricity in hydrogen form globally. The hydrogen will eventually compete with locally produced hydrogen and electricity [16].

To optimize lower transport costs, significantly more hydrogen needs to be produced than electricity. Wind and solar farms need to be sized based on hydrogen transport pipeline capacity, typically between 10-20 GW [17]. This volume of hydrogen production requires space for infrastructure, including solar/wind facilities, electrolyzers, compressors, cabling, pipelines, and access roads.

The hydrogen system is distinct from the energy system and will resemble the natural gas system. Gas provides necessary flexibility for both the electricity and hydrogen systems due to its larger production scale, transportation capacity, and storage capabilities. This transformation will likely turn regions like Europe, Japan, parts of the USA, China, and India into net hydrogen importers, while Australia,

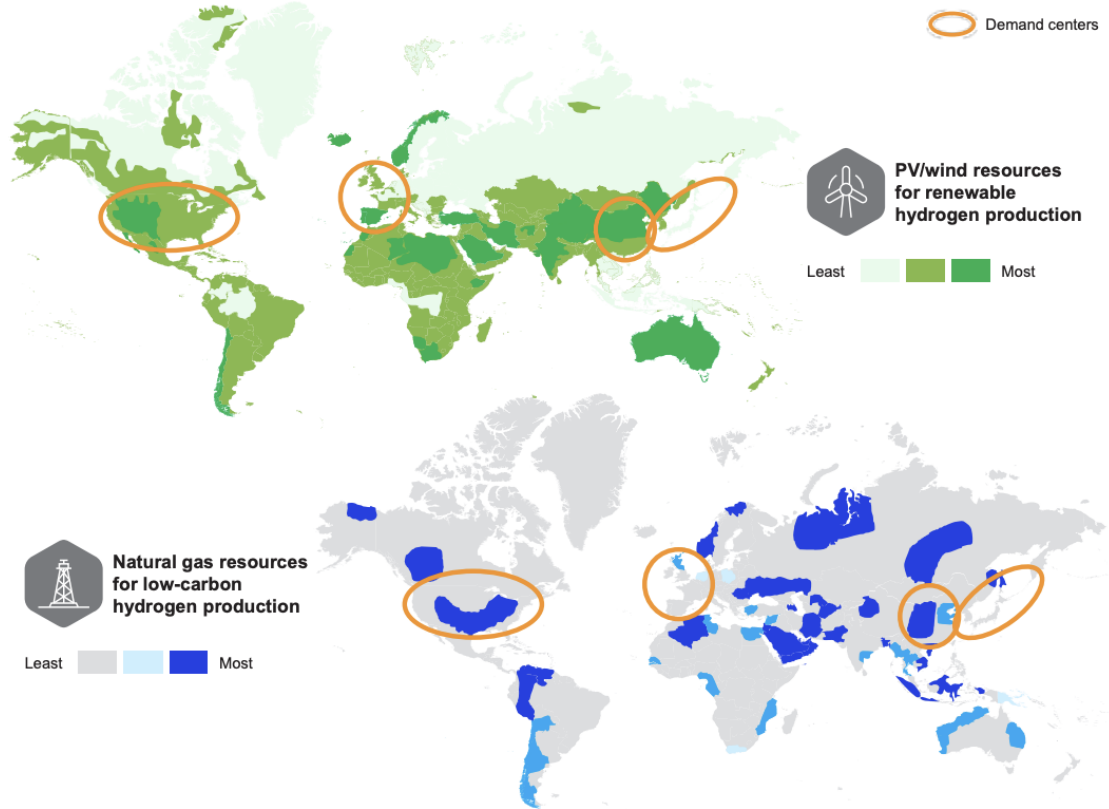


**Figure 1.4:** Global hydrogen resources and demand centers [16]

the Middle East, large parts of Africa, South America, and oceanic areas will become net hydrogen exporters.

### 1.3 Hydrogen transport and handling

The hydrogen integration into the gas system mentioned in section 1.2.2 comprises three pathways:

1. Injection and blending: involving the injection of hydrogen into the existing gas infrastructure and blending it with natural gas.
2. Dedicated hydrogen network: another approach is to establish a dedicated hydrogen network. This can be achieved by converting the existing gas infrastructure or constructing entirely new hydrogen infrastructure.
3. Methanation: entailing the  $CO_2$  capture and its combination with hydrogen to produce e-methane, which can then be injected into the gas network.

These pathways are complementary and depend on factors such as the production technology, geographical location, and project timelines. Presently, the gas infrastructure can accommodate various forms of low carbon hydrogen, regardless of the production technology used [18].

Hydrogen blending involves injecting a portion of hydrogen into the existing gas infrastructure alongside other gaseous energy carriers. In general, the capacity of the gas infrastructure remains largely unaffected by the level of hydrogen blending, with exceptions related to the injected share and specific applications [19].

Hydrogen deblending, on the other hand, is the process of separating pure hydrogen for dedicated purposes, such as hydrogen fuel cells and feedstock, as well as producing reasonably hydrogen-free natural gas. Key factors in choosing the appropriate technology include permeability, selectivity, membrane material stability, the impact of intermittent operation on the process, plant design, and the influence of hydrogen concentration in methane. Various membrane plant designs, in combination with different technologies like polymer, carbon, metal, glass/ceramic membranes, and membrane-PSA (Pressure Swing Adsorption), are utilized for hydrogen separation from gaseous energy carriers. Effective separation depends on the hydrogen concentration in the methane, and proper management of the separated hydrogen is crucial as discussed in section 2.4.

Hydrogen blending offers a straightforward entry point into the hydrogen economy, facilitating the rapid and decentralized deployment of renewable and low-carbon hydrogen technologies. It also allows for a centralized production scale-up. This approach can effectively reduce greenhouse gas emissions if hydrogen is produced from clean energy sources. In cases where pure hydrogen or methane is required, additional separation steps may be necessary.

Additionally, blending can serve as a cost-effective transitional solution, especially in regions lacking parallel or redundant gas networks or where available gas infrastructure can be readily repurposed for hydrogen in the short term.

Potential consumers of hydrogen blends are typically the same consumers who are currently connected to networks compatible with natural gas, including industries and domestic users who rely on gas heating. However, in specific instances, some end-users may not tolerate hydrogen admixtures beyond certain concentration levels. In such cases, gas quality handling technologies would be necessary to address these preferences and requirements [19].

The maximum allowable hydrogen concentration is primarily influenced by factors like pressure fluctuations, structural integrity, and pre-existing defects within the infrastructure. Current knowledge suggests that, for specific grid sections, blending percentages in the range of 2% to 10% in volumetric terms are technically feasible. However, it's important to note that further testing is required. Some operators are inclined to consider 20% as the upper limit given that downstream users would need to adapt beyond this threshold, which can pose challenges and lead to adjustments in their systems [20].

## 1.4 Scope and structure of the study

This master's thesis presents a comprehensive study on the deblending of hydrogen within the natural gas transmission network, with a specific focus on the Southern Sicily region. The research originates from an initial examination of the hydrogen landscape in Europe, emphasizing its integration into the gas network in alignment with European and non-European initiatives and regulations. The study progresses to the modeling of the Southern Sicily gas network using QGIS, employing data from Snam's website for network characteristics such as diameters, capacities, pressures, and delivery points.

The fluid dynamic simulation of gas within the network is conducted using the SIMPLE algorithm, both in its original form and modified to incorporate the deblending concept. Early in the thesis, deblending technologies are explored to enhance the understanding of their application in the later stages of the research. Each final node in the network is assigned a specific deblending method based on end-user characteristics. Following the reintroduction of hydrogen into the network, the study observes the gradual accumulation of hydrogen concentration within the pipelines, tracking its progression to the targeted industrial area in Southern Sicily.

This integrated approach, combining fluid dynamics simulation, deblending technologies, and network modeling, contributes to a comprehensive understanding of the complexities involved in the integration of hydrogen into the natural gas infrastructure. The research aims to provide insights into the behavior of gas mixtures, evaluate the application of deblending technologies, and assess the potential for enhancing the sustainability of energy transportation networks, with a particular emphasis on the Southern Sicily region.

## Chapter 2

# Hydrogen integration in the existing gas infrastructure

Today, hydrogen technology faces overcomable technical challenges, with ongoing advancements and digital solutions promising continuous improvements. Enhanced control over gas and electricity grids facilitates better alignment between renewable energy generation and diverse needs on national and global scales. Converting existing gas infrastructures to hydrogen operation holds significant potential for the hydrogen industry, exploiting current storage and transport capacities.

As a crucial element in the energy transition, hydrogen ensures a reliable energy supply during the shift to renewables, fostering swift and cost-effective progress in sector integration and power grid expansion. Simultaneously, long-distance gas networks pave the way for a global hydrogen market, connecting renewable energy-rich countries with diverse global markets efficiently. With widespread support from politics, industry, and the energy sector, hydrogen stands as a central energy source for the transition. The imperative now lies in consistently expanding renewable energy capacities and establishing a regulatory framework to guide the development of an efficient European and global hydrogen economy [21].

## 2.1 The European Hydrogen Backbone

Founded in 2020, the European Hydrogen Backbone (EHB) initiative initially included 11 Transmission System Operators and introduced a vision paper in July 2020 outlining a hydrogen transport infrastructure based on repurposing natural gas pipelines. Since then, the initiative has expanded to 33 network operators, covering 25 EU Member States, Norway, the United Kingdom, and Switzerland.



Figure 2.1: Companies participating in the EHB initiative [22]

The EHB’s vision underscores the technical and economic viability of a hydrogen pipeline infrastructure [23], aligning with the recognized role of hydrogen in achieving climate neutrality. This alignment is reinforced by the European Commission’s (EC) emphasis on hydrogen infrastructure in its December 2021 package [24], highlighting its importance for market competition, security of supply and demand.

Nonetheless recent events, including geopolitical shifts and the European Commission’s response in the form of the REPowerEU plan, underscore the imperative for a clean energy transition. REPowerEU aims to enhance the resilience of the European energy system by diversifying gas supplies and expediting the deployment of renewable gases and hydrogen [25]. The plan sets a target of achieving an additional 15 million tonnes (Mt) of renewable hydrogen, 5 Mt domestically produced and 10 Mt imported, beyond the 5.6 Mt outlined in Fit for 55, topping the EU’s hydrogen strategy targets [26].

The updated pan-European hydrogen network map for 2030 aligns with the EC’s goal to establish a 20.6 Mt renewable and low-carbon hydrogen market in Europe, as presented in the REPowerEU proposal.

The expansion of EHB maps reflects the EU’s growing climate ambitions, as

outlined in Fit for 55 and hydrogen packages. Vision maps also suggest potential locations for underground hydrogen storage, though these are indicative and do not yet consider simultaneous methane storage or the development of new storage sites. The proposed hydrogen backbone infrastructure is influenced by studies commissioned by the Gas for Climate consortium and the EHB initiative's 2021 study, emphasizing the substantial future role of hydrogen in a decarbonized European energy system. The vision acknowledges its dependence on future supply and demand dynamics, allowing for adjustments based on factors such as national policy discussions.

The establishment of dedicated hydrogen transport infrastructure hinges on market conditions, political support for hydrogen production and demand, and regulatory frameworks. The interconnected roles of LNG, biomethane, alternative pipeline gas, and hydrogen volumes add complexity, necessitating responsive and resilient infrastructure planning [26].

The EHB analysis revealed that a hydrogen pipeline has the capacity to transport approximately 65 TWh of hydrogen annually. To contextualize, this is half of the REPowerEU target of 10 Mt, equivalent to 330 TWh, necessitating around five large-scale pipeline corridors [26].

An initial analysis, considering supply potentials, demand centers, and assessments by Transmission System Operators on repurposing existing natural gas infrastructure and constructing new hydrogen pipelines, suggests the necessity of up to five supply corridors by 2030 [27]. The accelerated EHB network map in figure 2.2 illustrates these cross-border corridors, connecting regions with abundant solar resources in southern and eastern European countries and wind resources around the North, Baltic, and Mediterranean Seas. In areas with ample solar photovoltaic and wind potential, hybrid configurations offer a cost-competitive approach to hydrogen production.

The envisioned 2030 hydrogen infrastructure map, spanning approximately 28,000 km, aims to link these resource-rich regions to hydrogen consumers in central Europe. This connectivity becomes crucial as hydrogen adoption accelerates in transport, industry, and power sectors, leading to a demand that surpasses supply in regions with moderate renewable energy production potential. Additionally, these developments lay the groundwork for hydrogen pipeline imports from North Africa through Spain or Italy, from Ukraine through Poland, Slovakia, or Hungary, or through ship imports of hydrogen derivatives via planned new or repurposed import terminals.

In figure 2.2 five pan-European corridors aligned with the European Commission's REPowerEU goals can be identified:

1. Southern Europe Corridor: Expected to connect Tunisia and Algeria through Italy to central Europe, using existing natural gas networks. This corridor



**Figure 2.2:** Accelerated 2030 EHB network with its cross-border corridors [22]

could offer cost-competitive green hydrogen, supporting decarbonization along the transit route and Southern German clusters.

2. Iberian Peninsula Corridor: Envisioned for exporting green hydrogen from the Iberian Peninsula. New interconnections between Portugal, Spain, and France to Germany can play a crucial role in decarbonizing regional industries and transport.
3. North Sea Corridor: Emerging around the North Sea, linking offshore wind projects, hydrogen initiatives, and ship imports to industrial clusters and ports in the region.
4. Nordic and Baltic Corridor: Driven by onshore and offshore wind potential, this corridor aims to connect Nordic and Baltic hydrogen supply to the rest of Europe, supporting green projects and decarbonizing industries along the route.

5. East and South-East Europe Corridor: Connects hydrogen off-takers in Central Europe to regions with abundant renewable energy like Romania, Greece, and Ukraine. The region's land availability, high capacity factors for solar and wind, and potential repurposing of transit gas pipelines make it attractive for large-scale hydrogen production.

By 2030, hydrogen import strategies may involve both pipelines and terminals, depending on regional considerations and the pace of production scale-up [26]. Different regions may adopt varied approaches based on geopolitical situations. European Transmission System Operators (TSOs) are ready to deliver infrastructure to meet REPowerEU targets. As an example, the SunHyne Corridor, led by five major European gas transmission system operators - Snam, TAG, Eustream, NET4GAS, OGE - aims at facilitating the transportation of green hydrogen from North Africa to Germany, repurposing existing pipelines and establishing new infrastructure with the goal of importing 10 million tons of green hydrogen from third countries, aligning with the RepowerEU Package and the European Hydrogen Backbone.

### **2.1.1 Transmission System Operators**

Transmission System Operators face challenges that can be categorized into two main groups:

- Challenges related to TSOs' internal assets: this encompasses pipelines, valves, compressor units, turbines, simulation software, and other infrastructure owned by TSOs.
- Challenges associated with maintaining gas quality parameters at exit points: this involves ensuring specific gas quality standards at exit points leading to end-users, storage facilities, other TSOs, etc.

As the share of hydrogen (H<sub>2</sub>) in natural gas increases, challenges related to TSOs' internal assets become more pronounced, especially with fluctuations in the actual H<sub>2</sub> share. This impacts materials and the functioning of various components, with the interplay determining the minimum common denominator. These effects are crucial to consider when evaluating hydrogen's influence on TSOs' current assets and planning investments in new assets.

The subsequent points provide an outline and evaluation of the key components of the TSO network.

- In terms of steel pipelines, most exhibit commendable resilience against hydrogen, although a case-by-case assessment is crucial to address hydrogen

embrittlement effects. Potential solutions encompass adjusting design factors, implementing inner coatings, and monitoring, supported by integrity plans and modifications to transmission conditions. Notably, for a 2% vol.  $H_2$  concentration, pipeline steel generally proves suitable with negligible effects on entry and exit capacity [28].

- Moving to valves, both internal and external tightness are generally deemed non-critical for hydrogen concentrations up to 10% vol., as indicated by studies. While case-specific evaluations are necessary, there is an overall expectation of valves being suitable for a 2% vol.  $H_2$  scenario.
- In the realm of measurement tools, the readiness of gas chromatographs for 100% vol.  $H_2$  may necessitate upgrading for a 2% vol.  $H_2$  concentration. On the other hand, volume converters are generally deemed suitable for 2% vol.  $H_2$ , and existing flow measurement devices are expected to function adequately under the same conditions [21].
- When it comes to compressor stations, both compressors and compressor drivers (turbines) are generally deemed suitable for a 2% vol.  $H_2$  concentration, with minimal adjustments expected. Notably, drive power requirements for compressor units are typically slightly oversized for a 2% vol.  $H_2$  scenario. Looking ahead to 2030, standard compressor drive turbines are anticipated to operate seamlessly with up to 100% vol. hydrogen or undergo conversion accordingly. Additionally, ongoing development work suggests enhanced compatibility with hydrogen [18], indicating that standard compressor drive turbines may operate with up to 100% vol. hydrogen or be converted by 2030, showcasing the industry's commitment to evolving technology [29].

## 2.2 Hydrogen users and integration limitations

This section offers an overview of the current situation, highlighting the capabilities and limitations of each sector of users, along with the tools available in the market to address existing challenges.

As a starting point, a 2% volume of hydrogen is considered reasonable. While certain sectors can handle higher percentages, 2% serves as a common baseline because some industrial processes currently cannot manage more than this. It's important to recognize that the composition of connected customers to Distribution System Operators (DSOs) or Transmission System Operators (TSOs) varies significantly across Europe. Consequently, the eventual hydrogen blend transported or distributed will likely be determined for each grid section based on local structures, connected customers, and adherence to national technical rules and standards [30].

The building sector, representing 40% of final energy consumption and 36% of  $CO_2$  emissions in the EU, is a key challenge for decarbonization [31]. Heating and hot water production constitute 80% of a building's energy consumption, with nearly 60% of heating systems in Europe being outdated and inefficient, and 71% gas-based. The sector's transition to green gases is vital for meeting the EU's long-term climate goals. The existing heating stock can handle biomethane and varying methane-hydrogen blends, with boilers post-Gas Appliance Directive managing up to 10% vol. hydrogen [32]. Condensing boilers since 2005 can generally operate with up to 20% vol. hydrogen. Technologies for 100% vol. hydrogen appliances exist, defined as "20% vol. hydrogen appliance", "100% vol. hydrogen-ready appliance", and "100% vol. hydrogen appliance". These definitions are crucial for future-proofing appliances. Despite the capacity of current heating stock to handle blends, slow replacement rates - only 4% per year - hinder widespread green gas utilization, impeding the full decarbonization of building heat emissions [33].

Industrial appliances, contributing over 30% of gas consumption from public networks in the EU, can be categorized into three main groups [30]:

1. Medium and high power appliances for big buildings and district heating.
2. Medium and high power appliances supplying energy to industrial processes via hot water, steam, thermal oil, or other heat transmission fluids.
3. Small to high power appliances for the direct use of flue gas in industrial processes or methane as a raw material for chemical processes.

Understanding this classification is crucial for decarbonizing industrial gas appliances, considering their different sensitivities to gas quality:

- Group 1: Sensitive to gas quality but can tolerate limited variations, especially towards lower energy content.

- Group 2: More sensitive to gas quality to ensure required power output and temperature for connected industrial processes.
- Group 3: Highly sensitive to gas quality and tolerates almost no variation.

While the total number of industrial appliances is lower than household appliances, their substantial volume-based consumption emphasizes economic efficiency as a key driver for modernization and decarbonization in this segment.

For heating and cooking appliances, issues related to variations in gas quality and the handling of hydrogen are already noticeable. However, ongoing initiatives like THyGA (Testing Hydrogen Admixture for Gas Applications) are anticipated to furnish the necessary insights into challenges and potential solutions. Additionally, a project funded by the European Commission, aimed at "Eliminating the Technical Barriers to the Use of Hydrogen in Natural Gas Networks and for (Natural) Gas End Users", is scrutinizing the current scientific and technical framework concerning hydrogen utilization which will result in a gap analysis, subsequently translating into a set of pre-normative research (PNR) requirements. This endeavor aims to contribute to the standardization process for incorporating hydrogen into gas networks and for end users [30].

The main challenges in integrating hydrogen into gas networks include [18]:

- Measurement and metering: ensuring accurate measurement of hydrogen concentrations in gas streams and proper metering systems.
- Energy conversion: adapting energy conversion processes to accommodate hydrogen blending.
- Process gas chromatographs: implementing technology like process gas chromatographs to analyze gas composition.
- Interoperability across the EU: particularly addressing differences in blending levels across the European Union, which can hinder the interoperability of gas networks.
- Pressure loss along pipelines: dealing with pressure losses due to friction along pipelines, which need compensation through compressor stations.
- Compressor optimization: adapting compressors to hydrogen blends, considering that hydrogen has a lower molar weight than natural gas. Different compressor models respond differently to hydrogen blends, with some requiring replacement when hydrogen shares exceed 40% [21].

- Gas turbine compatibility: determining the compatibility of gas turbines, which often power compressors. While many new turbines can handle hydrogen blends, some may need modifications.
- Valves and underground storages: ensuring that valves and underground storage facilities can handle varying levels of hydrogen. While salt cavern storages are adaptable, research is ongoing for underground storages in porous rock.
- Material compatibility: assessing the effects of hydrogen on materials used in the infrastructure to ensure their integrity and safety.

More specifically, assessing whether existing pipelines can transport 100% hydrogen depends on the technical condition and chemical composition of the infrastructure materials. According to Gas for Climate, many existing natural gas pipelines are already suitable for hydrogen transport, and significant modifications may not be necessary [20].

For instance, under standard conditions, methane has three times the calorific heating value per cubic meter compared to hydrogen. Assuming the same operating pressure and pressure drop along the pipeline, hydrogen will flow at three times the velocity due to its lower density. Therefore, a gas pipeline designed for natural gas can transport about three times as many cubic meters of hydrogen during a given period, delivering a similar amount of energy. This results in only a slightly smaller energy transportation capacity compared to high-calorific natural gas. However, the assumption of the same operating pressures of  $H_2$  and  $CH_4$  may not be completely correct due to embrittlement issues, which will be further analyzed in the following sections [18].

The challenges abovementioned require careful consideration and, possibly, the development of appropriate solutions to enable the efficient integration of hydrogen into gas networks.

## **2.3 Hydrogen and natural gas blending**

The introduction of hydrogen expands TSOs' roles in gas quality management, potentially necessitating new tasks, responsibilities, and additional gas quality services. Challenges persist in agreeing on permissible hydrogen blending capacity within the system and across borders, requiring a delicate balance to preserve the freedom to trade gas.

The current landscape reflects a growing demand for the revision of gas quality standards at both entry and exit points. Gas suppliers often seek operational limit extensions at injection points, while end-users emphasize the importance of narrow and stable gas quality at exit points. This poses a technical challenge for TSOs as they navigate diverse requests while ensuring the seamless flow of gas across borders. It's noteworthy that the regulatory authority for gas quality standards lies within the national jurisdiction of each EU Member State [34].

Fluctuations in gas quality can stem from production-related and technical factors or alterations in the quantity of natural gas procured. Production-related variations result from shifts in the gas field, where the composition of gas extracted undergoes slight changes. These variations transpire over extended periods, spanning years and decades, without causing abrupt, significant fluctuations in the gas quality transported through the grid. On the other hand, technical-induced variations and shifts in the purchased amounts can lead to substantial and sudden effects, impacting end users both technically and economically. These variations may occur, for instance, when gases from different gas fields are blended in the grid or when gas from a new source is introduced into the grid [30].

Effective collaboration among TSOs is essential to address these challenges and prevent potential cross-border restrictions, along with the need for long-term flexibility in gas quality standards to ensure the integrity of gas networks and the smooth functioning of the internal gas market [35]. However, the optimal decarbonization strategy varies based on local factors, leading to a gap between technical possibilities and legal allowances. Organizations like Marcogaz, GERG, and CEN, along with projects, actively explore gas infrastructure and end-use applications regarding allowable hydrogen content.

The European Commission-funded project, "Removing the technical barriers to the use of hydrogen in natural gas networks and for (natural) gas end-users," contributes to standardization by identifying gaps and proposing pre-normative research requirements. At the cross-border level, under the Interoperability Network Code (INT NC), TSOs establish bilateral Interconnection Agreements (IAs) defining operational rules at interconnection points (IPs). While the INT NC doesn't mandate gas quality specifications in IAs, many TSOs have included such specifications. However, hydrogen is not commonly listed among the parameters subject to specifications in current Interconnection Agreements. A revision of

these agreements would be necessary to facilitate the safe and efficient cross-border transport of hydrogen in the future [30].

The introduction of hydrogen into natural gas grids can significantly impact the system, influencing factors such as relative density, calorific value, Wobbe Index, flame speed, and combustion temperature. These modifications, particularly in the Wobbe Index, relative density and higher heating value range, may constrain the operational window for end-use applications, especially those adjusted for higher hydrogen shares. Ensuring greater gas quality stability than current standards is crucial in this context.

The following definitions refer to the three most important parameters to be considered and evaluated in this work:

Methane-hydrogen gas blends, distinct from pure methane or hydrogen, exhibit altered physical properties and combustion characteristics. The density of such mixtures is lower than pure methane, leading to increased gas leakage volumetric flow rates [11]. Viscosity notably decreases when hydrogen concentration exceeds 50%. The lower heating values (LHV) increase slightly with higher hydrogen content, but pure hydrogen has LHV values over two times higher than any methane-hydrogen mixture with up to 90% hydrogen. These differences influence flow behavior and energy transport efficiency in pipeline transportation [36].

The main properties of the two gases are shown in table 2.1.

Property	Hydrogen	Methane	Unit
Molar Mass	2.02	16.04	<i>g/mole</i>
Specific heat capacity $T = 293 K$ and $P = const$	14.4	2.21	<i>kJ/kg/K</i>
Critical Temperature	33.2	190.65	<i>K</i>
Critical Pressure	13.15	45.4	<i>bar</i>
Steam density $T = 293 K$ and $P = 1bar$	0.0838	0.651	<i>kg/m<sup>3</sup></i>
Mass lower calorific value	120	48	<i>MJ/kg</i>
Volume lower calorific value @1 atm	11	35	<i>MJ/m<sup>3</sup></i>
Maximum flame temperature	1800	1495	<i>K</i>
Explosion limit	18.2-5809	5.7-14	<i>Vol%inair</i>

**Table 2.1:** Property comparison of hydrogen and methane [37]

---

Hydrogen blending, often associated with power-to-gas installations, is expected to increase intermittently. While current limitations on hydrogen fractions may not significantly impact gas quality variability, higher concentrations could widen local ranges, affecting end-use applications and the gas infrastructure. Despite challenges,

hydrogen injection is recognized as a pivotal enabler for a nearly carbon-neutral future.

In a hydrogen-blended environment, the interaction between hydrogen and pipes leads to the degradation of mechanical properties such as hardness, plasticity, and toughness. This degradation poses a significant challenge to the safety of pipelines. While hydrogen-blended natural gas exhibits high compatibility with traditional non-metallic materials, it can cause hydrogen damage to metal components in natural gas transportation systems, jeopardizing the safe operation of pipelines. For this reason, research on pipe compatibility primarily focuses on metal materials due to the manifestation patterns of hydrogen damage, including hydrogen embrittlement, hydrogen-induced cracking, and hydrogen bubbling, with hydrogen embrittlement posing the greatest risk [37].

Hydrogen-induced cracking and hydrogen bubbling are two forms of hydrogen damage caused by the combined action of hydrogen atoms and molecules without external force. These manifestations involve hydrogen atoms entering the metal interior, gathering into hydrogen molecules at defect sites, and inducing dislocations and failures in the metal

Hydrogen embrittlement, on the other hand, poses more serious harm by dissolving hydrogen atoms in the metal lattice, producing massive defects, and significantly reducing the ductility and tensile strength of the materials. Hydrogen embrittlement can initiate cracks and induce failure even without external force, making it a critical concern.

Research on hydrogen embrittlement spans microscopic and macroscopic perspectives. At the microscopic level, studies employ methods such as the molecular dynamics method and electron microscopy to understand the failure mechanisms and changes in the microstructure of materials in a hydrogen-rich environment. These studies reveal mechanisms like hydrogen atom diffusion, lattice distortion, and their effects on material properties. At the macroscopic level, research focuses on testing the mechanical properties of materials in a hydrogen environment, including tensile properties, fatigue properties, fracture toughness, and crack propagation. These tests provide essential parameters for pipeline design and operation [37].

Variations in hydrogen concentration, service conditions, and pipeline defects can influence the susceptibility of pipelines to hydrogen embrittlement [38]. Furthermore, hydrogen significantly influences the weld seam of pipe section joints, with residual stress identified as a main contributor to hydrogen enrichment and embrittlement failure. Prevention and control measures for hydrogen embrittlement involve considerations such as steel grade, the introduction of *CO* to inhibit embrittlement, and the development of preventive coatings on the inner wall of pipelines. However, these measures are often more applicable to new pipelines than existing ones. Reducing gas pressure or controlling the hydrogen blending ratio is recommended

to ensure transportation safety, though it may impact the capacity and efficiency of pipeline hydrogen transportation [37].

In end-user applications, burners with 0-30% hydrogen-blended methane-hydrogen mixtures showed no flashback or flame life issues, with only a 1-1.5% change in overall burner efficiency. Above 25% hydrogen, burner tube flashback became a limiting factor in commercial oven burners [39]. In a gas turbine engine designed for natural gas, low hydrogen content raised flame temperature, favoring combustion efficiency, but as hydrogen concentration increased, engine power shortage occurred due to reduced mass flow rate of fuel. Testing methane-hydrogen mixtures in a fuel cell showed no significant difference between pure hydrogen and 5% hydrogen injection in methane, concluding that diluted hydrogen fuel is as energy-efficient as pure hydrogen [36].

In natural gas networks, lower energy quantity is transported with increasing hydrogen volume percentage in methane-hydrogen mixtures, requiring more compressor stations. Hydrogen with volume fractions up to 20% fits existing infrastructure with minor modifications, but above 30%, additional compression stations and polyethylene pipelines are required [40]. Instability and reduced pipeline efficiency were observed when hydrogen concentration exceeded 30% in an existing natural gas network. A methane-hydrogen pipeline system showed reduced gas mixture relative density and heating values.

The introduction of hydrogen in natural gas pipelines also altered thermodynamic transport conditions, affecting explosion severity. Hydrogen, due to lower density and higher sonic speed, traveled farther from the pipeline, decreasing ignition chance and flame acceleration.

Regarding energy transport efficiency, a 10 vol% hydrogen methane-hydrogen mixture self-consumes almost two times more energy than natural gas during transportation. Energy costs for transporting hydrogen blends depend on hydrogen volume fraction and flow conditions, with the lowest costs for pure hydrogen and the highest for hydrogen transported at the same mass flow rate as methane. However, a detailed study of the cost of transporting methane-hydrogen gas blends across various parts of the pipeline infrastructure is not yet available [36].

## 2.4 Hydrogen deblending

Blending hydrogen into the existing natural gas pipeline network has been proposed as a method for transporting low-carbon energy. Therefore, a transitional solution is needed to achieve a 100% hydrogen future network.

Deblending, which consists in separating the blended gas stream, is a potential solution to allow the existing gas transmission and distribution network infrastructure to transport energy as a blended gas stream. Deblending can provide hydrogen, natural gas, or a blended gas for space heating, the transport industry, and power generation applications. If proven technically and economically feasible, utilizing the existing gas transmission and distribution networks in this manner could avoid the need for investment in separate gas and hydrogen pipeline networks during the transition to a fully decarbonized gas network.

Gas separation technologies, such as cryogenic separation, membrane separation, and Pressure Swing Adsorption (PSA), are well-established and mature, having been used and proven in natural gas processing for decades. The mentioned technologies require energy input to drive the separation of gas components. The configuration of the gas transmission and distribution networks provides a possible source of available energy through the pressure let-down in the network pressure tiers, which could be used to drive the gas component separation processes.

Following hydrogen separation, the residue gas could be re-injected into the gas networks operating at low pressure, reducing energy requirements associated with recompression. The process performance and economics benefit from the availability of large pressure differentials and the low operating pressure of downstream networks. The techno-economic case for deblending is heavily influenced by the available network operating conditions, such as pressure differentials and operating pressure of downstream networks, hydrogen content in the gas blend, and capacity. Feasibility is also influenced by particular site conditions, such as network configuration, network operation dynamics, and site constraints. Further study work will be required to ascertain the scalability and potential deblending could play in decarbonizing the gas system [41].

Figure 2.3, for completeness, summarizes the main hydrogen separation technologies with their respective characteristics and operating conditions.

Technology	Capacity (scale)	Typical feed H <sub>2</sub> content	Typical feed pressure (barg)	Typical feed temp (°C)	Hydrogen product pressure	Residue gas pressure	Hydrogen recovery (mol%)	Hydrogen purity (mol%)
PSA	Large	>50%	10-150	0-40 (amb)	High (feed pressure)	Low (atm)	80-90%	99.7% (99.999% max)
Polymer membrane	Small to medium	>20%	20-200	0-40 (amb)	Low (2-3 barg)	High (feed pressure)	70-90%	50-98% (99.7% max)
Palladium membrane	Small	>98%	<20	300-450	Low (2-3 barg)	High (feed pressure)	95-99%	99.5-99.995%
Cryogenic	Large	>20%	20-50	0-40 (amb)	High (feed pressure)	Low (2-3 barg)	80-90%	90-98%
EHS	Small	>10%	3-15	0-40 (amb)	High (higher than feed)	High (feed pressure)	<95%	99.999%

**Figure 2.3:** Main hydrogen separation technologies [41]

Polymeric membrane, cryogenic, and Pressure Swing Adsorption (PSA) technologies have been selected for the deblending process. These technologies are chosen based on their maturity, proven track record, and the availability of a large number of suppliers, ensuring that the deblending process can be implemented with proven and readily available solutions.

### 2.4.1 Pressure Swing Adsorption

Pressure Swing Adsorption (PSA) is a well-established technology that features extensive design and operational expertise, employing optimized bed switching sequence control to enhance hydrogen recovery. In PSA units, gas components are separated from hydrogen through adsorption at high pressure, resulting in a purified hydrogen stream exiting the unit at an elevated pressure, typically reaching 99.7 mol% and potentially as high as 99.999 mol%.

Operating on adsorption isotherms, PSA relies on the physical adsorption of non-hydrogen gases on media, utilizing porous adsorbent materials. Hydrogen, being highly volatile and low in polarity, is practically non-adsorbable, making PSA ideal for hydrogen purification. Regeneration involves reducing the adsorbent bed pressure from an elevated operating pressure to slightly above atmospheric pressure, utilizing the swing in pressure that gives the technology its name. Beds are regenerated by isolating a specific bed, depressurizing it, and using a portion of the hydrogen product as a sweep gas to enhance desorption.

A minimum of four adsorber vessels is essential for adsorption, depressurization, regeneration, and re-pressurization. As illustrated in figure 2.4, only one bed is in duty at any given time, while others are in varying steps of the regeneration cycle. A typical cycle time for a PSA unit is approximately 10 minutes, with shorter cycle

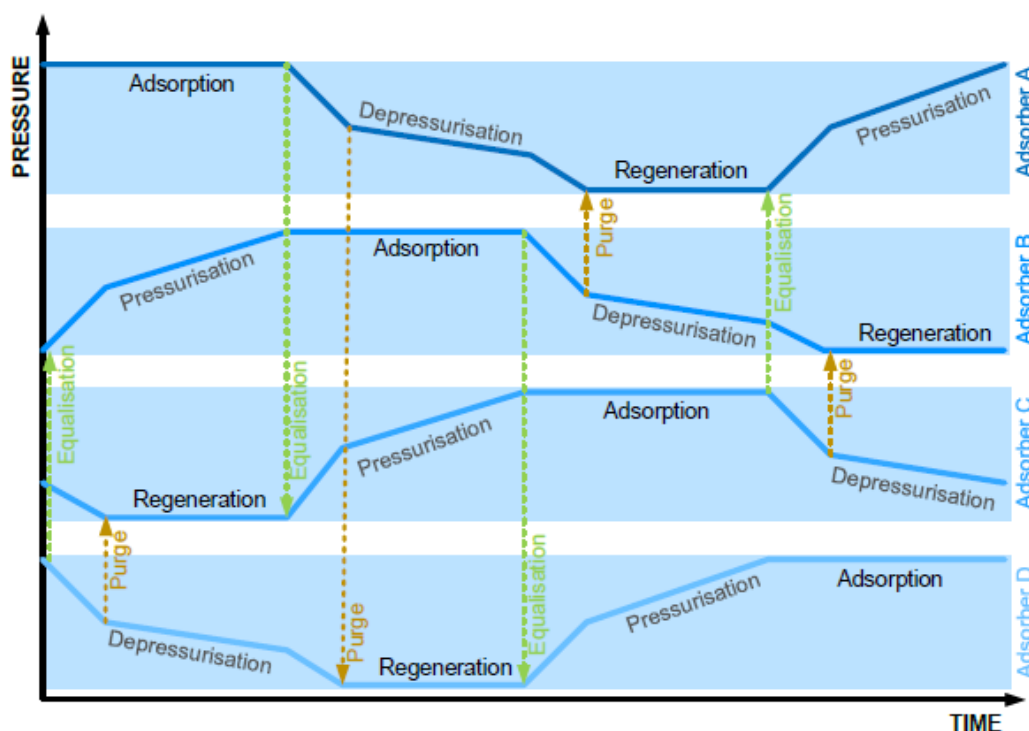


**Figure 2.4:** Typical Pressure Swing Adsorption cycle [41]

times of less than 30 seconds, known as Rapid PSA, now commonplace [42]. In such systems, automated valve opening and closure with tightly timed sequence control become crucial, facilitated by the use of rotary multiport valves for multiple simultaneous changeovers in all the columns.

PSA technology, widely adopted globally, is primarily used for hydrogen purification, achieving high purity levels ranging from 99.7 mol% to as high as 99.999 mol%. Hydrogen production occurs at high pressure, typically 10 to 40 barg, with capacity reaching up to approximately 10 million cubic meters per day, although multiple vessels or parallel PSA units can be employed for scalability [43].

Recovery rates typically range between 80-90%, with short adsorption cycles lasting seconds to minutes. Adsorber bed size depends on factors like feed gas flow, hydrogen feed content, and required product purity. If hydrogen content decreases or higher purity is needed, the bed size and the number of beds may increase.

Residue gas is produced at low pressure (<0.5 barg nominal), often requiring nearby low-pressure fuel gas users for disposal. PSA is generally not used for feed gas containing less than 50 mol% hydrogen due to recompression duties [41]. To address this, upstream processing technologies like membranes can concentrate hydrogen, reducing the volume of residue gas from the PSA.

## 2.4.2 Polymeric membrane separation

Membrane technology utilizes tubular hollow fiber polymeric membranes arranged in modules for gas separation, increasing capacity by adding modules. Operating on selective permeation principles, the membranes consist of a non-porous film facilitating gas transport through the solution diffusion mechanism. Gases with low molecular weight, such as hydrogen, and strong polarity exhibit high permeabilities. The resulting hydrogen product permeates through the membrane at low pressure. Membrane units are constructed from various materials, including conventional polymeric hollow fibers (polysulfone, aromatic polyamides) and non-polymeric materials like molecular sieving carbon, zeolites, and ceramics.

Polymeric membranes can be rubbery or glassy, with rubbery polymers having high permeabilities and glassy polymers exhibiting high selectivity. Conventional membranes, robust and suitable for hydrogen content feed gas as low as 20 mol%, may use strategies like increased module size or feed pressure to enhance hydrogen recovery. Alternatively, a two-stage membrane process involves recycling a portion of purified hydrogen to concentrate hydrogen content in the feed gas. A typical polymeric membrane separation process is illustrated in figure 2.5.

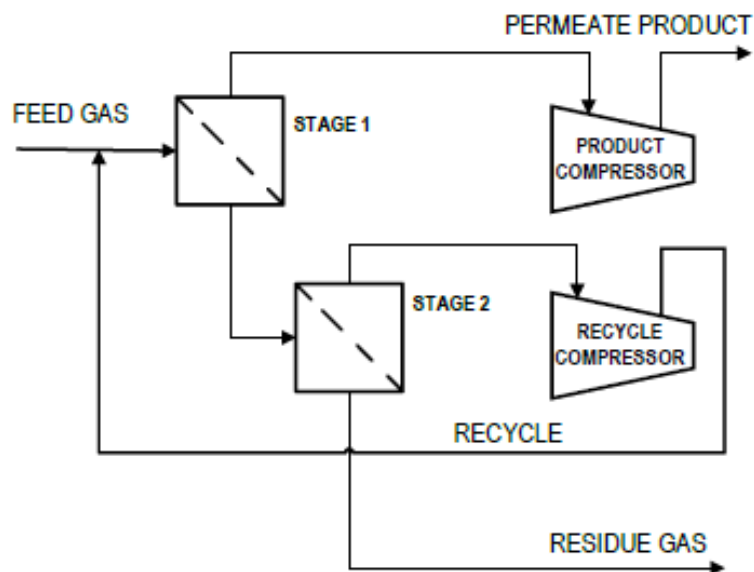


**Figure 2.5:** Typical Membrane separation flowsheet [41]

Processing low hydrogen content feed gas may require additional energy for recycle recompression.



Internally, a combination of aluminum and stainless steel is used, and specially designed thermal shunts protect the structure from extreme cold. The process involves continuous purging with dry nitrogen to maintain a safe atmosphere within the cold box housing.

Cryogenic separation is notable for its efficiency and safety, making it a crucial technology in hydrogen purification within industrial settings, particularly in midstream gas processing and the petrochemical sector. It requires meticulous feed gas pre-treatment to eliminate impurities like  $CO_2$ ,  $H_2S$ , water, and mercury. This mature technology, with a high Technology Readiness Level of 8 to 9, is suitable at handling feed gas with a hydrogen content exceeding 50 mol% and can achieve hydrogen purities as high as 98-99 mol%.

Operating examples often involve ambient temperature and high-pressure feed gas, making cryogenic separation suitable for bulk hydrogen separation. It yields a high-purity hydrogen-rich stream at high pressure, with typical hydrogen purity ranging from 90-95 mol%, potentially reaching as high as 98-99 mol%. The technology boasts a typical hydrogen recovery rate of around 80-90% without requiring external refrigeration, as refrigeration is generated by the pressure let-down of natural gas product streams [41].

# Chapter 3

## Methodology

This chapter serves as a guide to the strategic decisions and technical processes backing the research, offering a transparent and systematic account of the methodology employed in the exploration of hydrogen integration dynamics within the natural gas infrastructure in the Southern Sicily region.

Beginning with an explanation on the motivation behind selecting the Southern Sicily region as the focal point, this chapter proceeds to unveil the stages of modeling the gas network using QGIS. A detailed account of the data selection process sheds light on how parameters such as capacities, diameters, pressures, and delivery points were extracted from Snam's website, ensuring a fair grade of accuracy and relevance of the model.

The methodology further explores the specifics of the fluid dynamic simulation process, illustrating the utilization of the SIMPLE algorithm tailored to capture the dynamics of hydrogen blending and debinding within the transmission network. A comprehensive explanation of the model's implementation provides readers with a clear understanding of the simulation framework employed to analyze the behavior of gas mixtures.

### 3.1 Case study selection

The selection of the southeastern region of Sicily as the primary focus for this thesis is grounded in several strategically significant considerations.

Sicily, serving as a critical gateway for natural gas imported from Algeria and Libya through the Transmed and Greenstream pipelines, establishes a pivotal connection between North Africa and Italy, facilitating the subsequent distribution of gas throughout Europe. As elucidated in section ??, the North African region exhibits a heightened propensity for electricity production from renewable sources, fostering the favorable conditions for the production of green hydrogen. This green hydrogen

can be seamlessly integrated into the gas transmission network, thereby functioning as an energy carrier.

Furthermore, the active participation of the Italian Transmission System Operator, Snam, in the European Hydrogen Backbone initiative, coupled with their expressed intention to integrate hydrogen into the network through the Sunshyne Corridor project as mentioned in section 2.1, underscores the strategic importance of the chosen region.

Snam is a key player in Italy’s hydrogen strategy, with an extensive transportation network of over 32500 km and a storage capacity of 17 billion cubic meters [26].



**Figure 3.1:** National Transmission System in Italy [26]

Snam’s infrastructure plays a crucial role in facilitating the integration and distribution of hydrogen across the country.

As illustrated in figure 3.1, the national backbone connects industrial clusters in the North and some areas in the South to green and blue hydrogen production facilities in the Centre, South, and potentially North Africa.

Development is likely to involve a shift from fossil sources to hydrogen, utilizing retrofitted existing natural gas pipelines. Parallel routes and extended grid infrastructure will support the scalability of the hydrogen industry.

As the hydrogen industry scales up and costs decrease, the grid will undergo further extensions to connect with additional markets. The goal is to establish Italy as

a key player in Europe’s hydrogen supply chain. Snam’s extensive infrastructure and strategic positioning align with Italy’s ambitions to integrate hydrogen into its energy landscape, fostering green and low carbon hydrogen production, distribution, and international connectivity.

Italy’s national hydrogen strategy targets 2% of the country’s final energy demand from hydrogen by 2030, as outlined in national guidelines. Concentration of demand is expected in industrial clusters, particularly in the North, with potential growth in hydrogen valleys in the South, especially Sicily and Puglia regions [26].

The southeast of Sicily is particularly relevant to this thesis’s objectives, as it aims to scrutinize the separation and subsequent accumulation of hydrogen within the transmission network through reinjection. Given the aim to accumulate higher quantities of hydrogen for industrial applications, especially within refineries, as explicated in preceding chapters, the selection of this region becomes crucial.

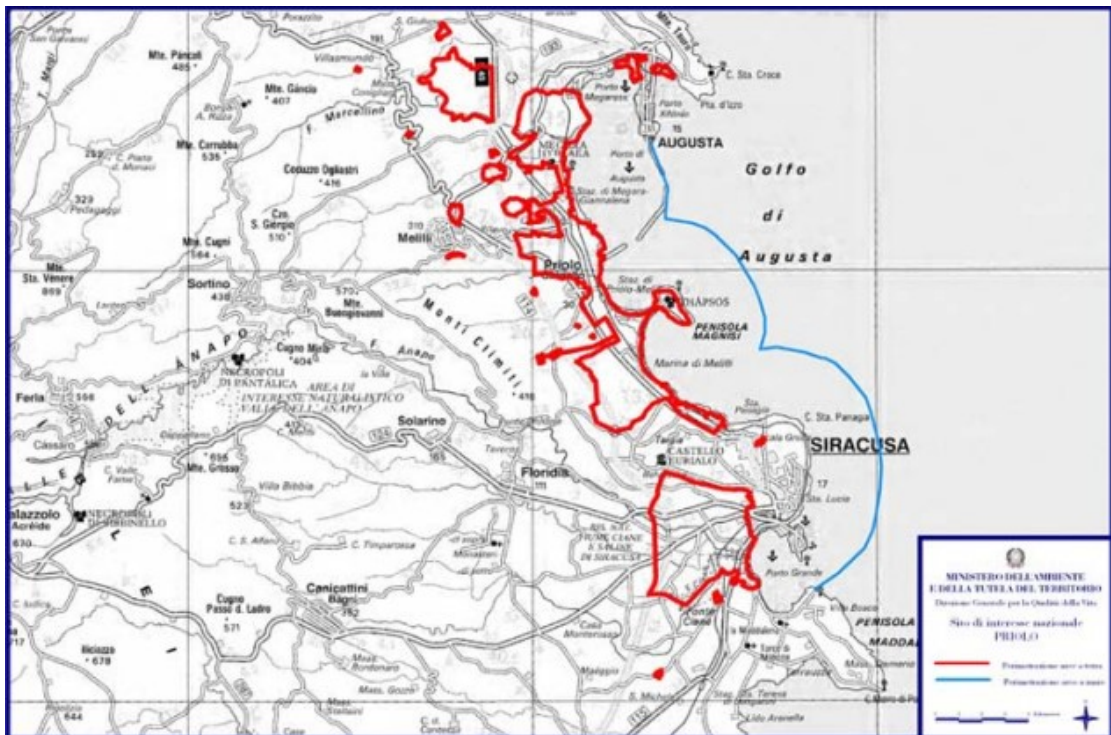


**Figure 3.2:** Syracuse petrochemical hub [44]

The presence of the "Syracuse Petrochemical Hub" represents a significant industrial complex in eastern Sicily, encompassing the municipalities of Augusta, Priolo Gargallo, and Melilli, extending to the suburban area of Syracuse. This extensive coastal area is characterized by industrial activities primarily focused on petroleum refining, the processing of its derivatives, and energy production.

Among the major facilities contributing to the complexity of this industrial settlement are the refineries operated by Sonatrach (formerly Esso) and the ISAB Refinery, including both south and north plants, originally known as ERG, AGIP, and ISAB. Additionally, noteworthy chemical plants include those managed by Eni Versalis, Sasol, and Eni Rewind (formerly EniChem Augusta Spa). Other significant installations comprehend the Isab Energy Gasification and Cogeneration Plant, Air Liquide Italia Produzione, specializing in the production of liquefied gases, the currently inactive Sardamag Magnesite Factory, the Augusta Cement Plant, the Industrial and Civil Sewage Treatment Plant IAS, and the Enel Archimede Power Plant. The combination of these facilities significantly contributes to the industrial landscape of the region, forming a complex network of activities with substantial impacts on local economic development.

The presence of this hub aligns with the research's focus on understanding the dynamics of hydrogen integration in a context highly relevant to industrial processes.

## **3.2 Network modelling and data preparation**

This section includes an examination of the process of network modeling and data preparation, explaining the conversion of the Sicilian Snam network representation into a precisely georeferenced topology through QGIS. The primary aim is to achieve a high level of precision and coherency in the modeling process, referring to the existing TSO infrastructure. Employing georeferencing techniques within QGIS serves to authentically replicate the network's topology, forming a robust foundation for the simulations and comprehensive analyses.

Subsequently, attention is directed towards the extraction of publicly available data shared by Snam, specifically focusing on the Italian gas network. Essential parameters, including entry points into the network and delivery points, are extracted to establish an adequate dataset, crucial for the execution of simulations.

### 3.2.1 Network modeling through QGIS

The network modeling employed in this study reflects a methodological approach centered on the application of Quantum Geographic Information System (QGIS), a Geographic Information System (GIS) tool. At its core, the modeling began with the task of georeferencing the Sicilian transmission network representation in figure 3.3 obtained from Snam website through the *Georeference* tool.

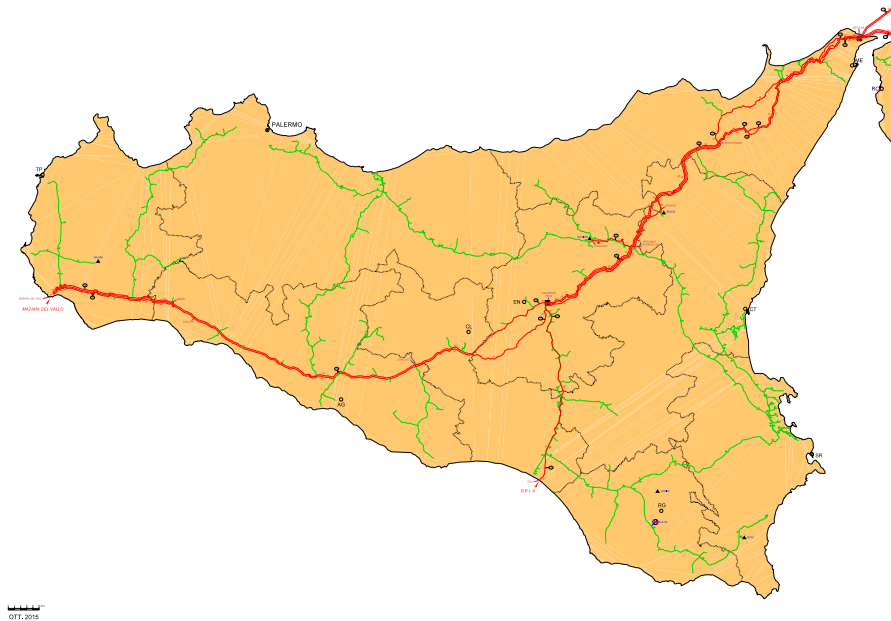


**Figure 3.3:** Sicilian Transmission Network representation [45]

The precision achieved in this process, with spatial accuracy maintained below 300 meters, underscores the careful overlay mechanism. Within the QGIS framework, the construction of the network unfolded organically, by creating a new shapefile layer on which the new digitalized network has been designed, facilitated by the use of the *line* tool. The alignment of line initiation and termination points with the network's nodal intersections and branching points was crucial in capturing the network's topological intricacies. For the purpose of this study, only the part of the network affecting the area covered in the previous section was modeled, as shown in figure 3.4.

The two types of network, as categorized by the TSO, can be seen: the National network, shown in red, and the Regional network, shown in green. The end nodes, corresponding to the redelivery points discussed in more detail in the next paragraph, are represented as points.

In the course of network creation, an attribute table was compiled, detailing the

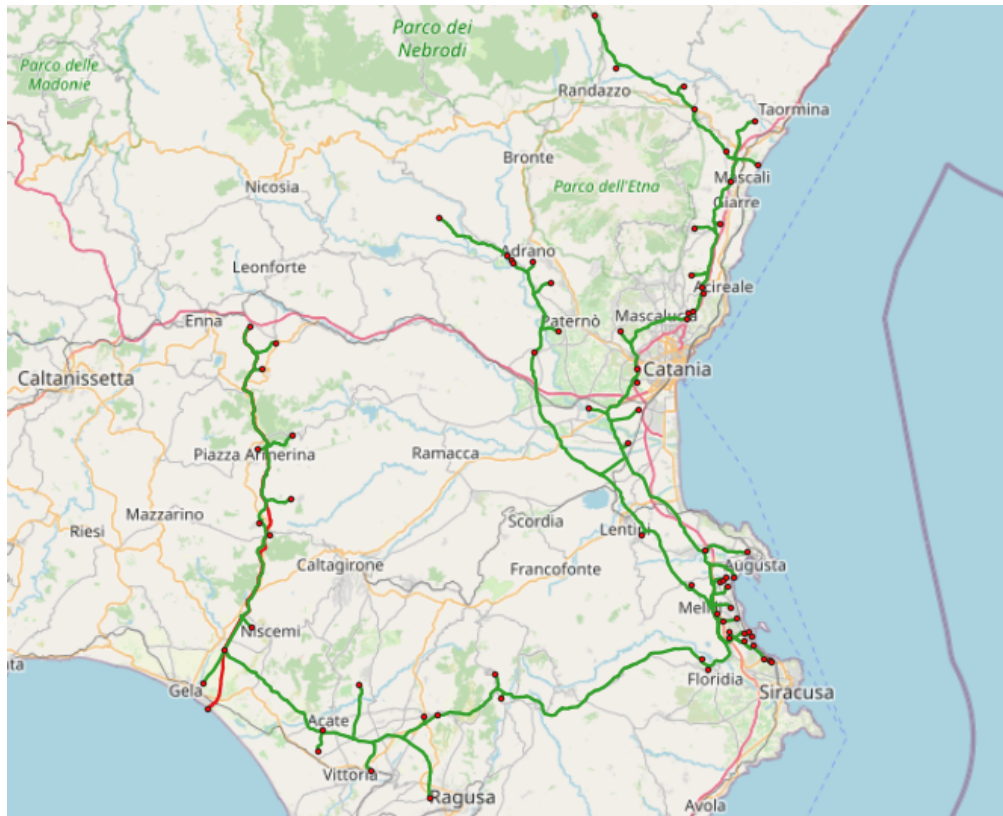


**Figure 3.4:** Sicilian reduced Transmission Network model representation

characteristics of each individual line. Diameters were assigned, sourced from available cartographies with cross-references to the Snam database to ensure data accuracy, and systematically recorded for each line [46]. The classification of lines into regional or national categories was specified, each with its corresponding surface roughness parameters. An addition to this table is the inclusion of a network segment, symbolic of a connection between the national and regional networks and representative of a pressure reduction facility.

Furthermore, the precise calculation of section lengths was facilitated using QGIS's calculation tool. This length data is instrumental for the upcoming fluid dynamic simulation, to be discussed in subsequent sections.

The resultant network, particularly its attribute table, contains geographic information essential for the unfolding stages of this study. Upon its integration into MATLAB, exploiting the information derived from QGIS, the dataset assumes a pivotal role in constructing an adequate network topology, setting the stage for the forthcoming simulations. The table 3.1 summarizes some of the results of the network topology import in MATLAB to give an idea of the data elaboration

computed.

Node ID	X Coordinate	Y Coordinate	Degree
1	4449819.63904633	1589568.39223373	1
2	4444919.68294869	1590391.49632808	1
3	4456199.85023494	1593740.43313106	4
4	4456134.19595984	1593748.99818682	3
5	4462640.10059642	1596852.23611897	3
6	4517440.21469403	1598342.96070069	2
7	4517458.55716054	1598366.68643105	3
8	4517464.42393434	1598412.44726672	1
9	4460552.74729958	1598883.28499881	1
10	4509488.50695782	1599322.89840337	3
11	4512581.79412686	1599400.54402456	3
12	4494429.21571546	1600093.19575572	1
13	4480151.21420386	1600386.13263119	1
14	4480859.48304297	1600603.45238680	3
15	4509439.01612279	1600722.93913657	1
16	4484617.26715702	1601450.95544179	3
17	4494671.83078674	1601463.98190643	4
18	4478320.93314480	1601785.95340513	3
...	...	...	...
147	4556625.40139808	1694168.47899951	1
148	4548072.92556165	1694808.44925974	1
149	4454457.15046873	1695975.83541216	1
150	4454532.63002263	1696009.56031922	3
151	4453991.42556167	1697159.41905528	3
152	4454089.38838695	1697173.87258688	1
153	4453800.31775498	1697392.28150882	1

**Table 3.1:** Nodes' Coordinates X and Y

With reference to table 3.1, it is important to note that the coordinates are presented in an X-Y reference system. Additionally, the fourth column of the table indicates the nodes' degree, which represents the number of connections or edges that the particular node has with other nodes in the network.

In the following, it will be clear how grade one nodes will take on particular importance during the course of the simulations.

Table 3.2, instead, presents the result of MATLAB elaboration of the network topology, in particular the transformation of the lines created in QGIS into network

edges characterized by entry and exit nodes. Additionally, the table illustrates other useful information such as line characterization, assigned diameters and pipe lengths.

<b>Node In</b>	<b>Node Out</b>	<b>Type</b>	<b>D [m]</b>	<b>Length [m]</b>
1	3	Rete Regionale	0.5	6162
2	4	Rete Nazionale	0.9	9892
3	5	Rete Regionale	0.75	5804
3	24	Rete Regionale	0.6	21245
4	7	Rete Nazionale	0.9	56266
5	9	Rete Regionale	0.1	2370
5	18	Rete Regionale	0.75	15009
6	11	Rete Regionale	0.4	4779
7	8	Rete Nazionale	1.2	37
10	11	Rete Regionale	0.4	2649
10	15	Rete Regionale	0.1	1155
10	17	Rete Regionale	0.4	14291
11	20	Rete Regionale	0.1	4256
12	17	Rete Regionale	0.1	1244
13	14	Rete Regionale	0.1	605
14	16	Rete Regionale	0.4	3622
14	18	Rete Regionale	0.4	2454
16	17	Rete Regionale	0.4	8640
...	...	...	...	...
145	146	Rete Regionale	0.1	123
145	150	Rete Regionale	0.25	2724
149	150	Rete Regionale	0.1	66
150	151	Rete Regionale	0.2	1017
151	152	Rete Regionale	0.1	79
151	153	Rete Regionale	0.2	240

**Table 3.2:** Branches data

---

As shown in figure 3.5, a check has been made on the accuracy and completeness of the network, ensuring that all nodes are linked together.

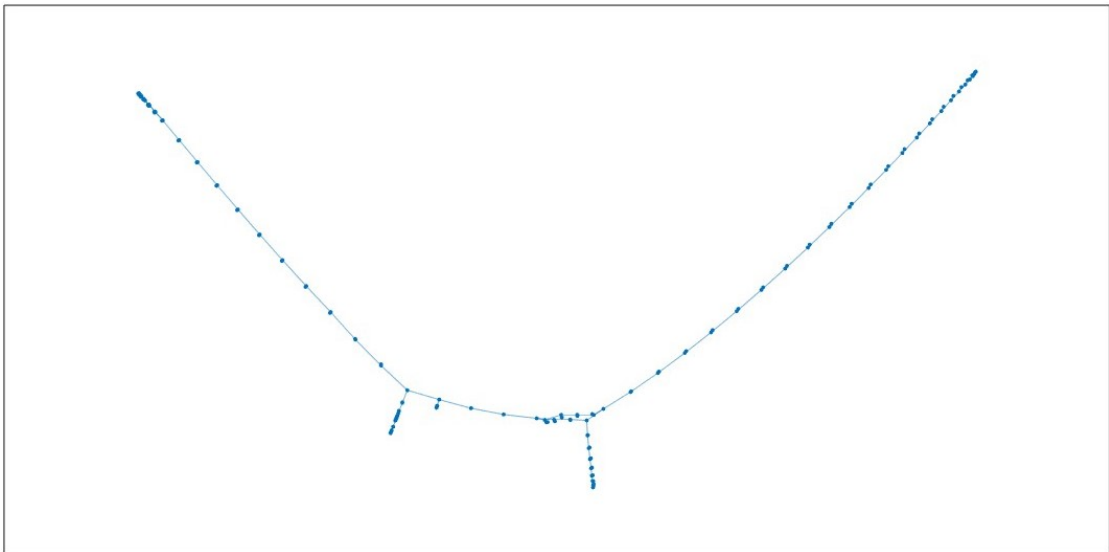


**Figure 3.5:** Sicilian reduced Transmission Network model check on MATLAB

As presented in figure 3.6, the embedded geographical coordinates serve not only as a visual aid, but also as key identifiers for network nodes which will assist the data preparation process covered in the next section.

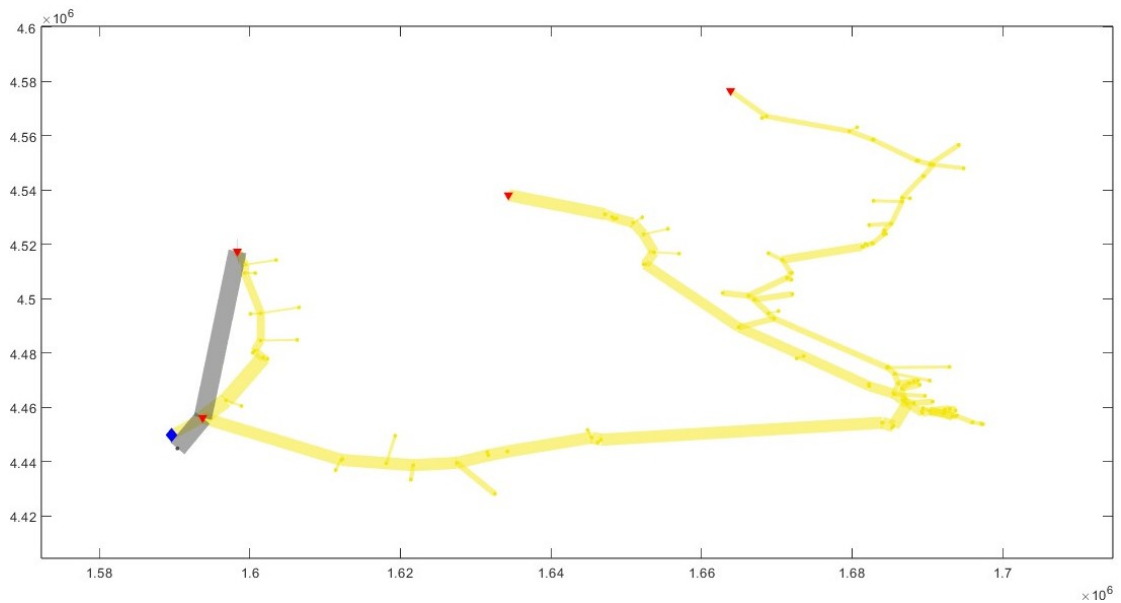


**Figure 3.6:** Sicilian reduced Transmission Network model on MATLAB, considering coordinates

### 3.2.2 Data preparation

The acquisition of fundamental data for carrying out the fluid dynamic analyses discussed below was done by exploiting the databases made public on the Snam website. Specifically, the dataset concerning the thermal year 2023, was employed to collect insights into monthly capacities and gas pipeline pressures [47]. This comprehensive repository encompasses delivery points across Italy, each of them identified by unique codes, their associated municipalities, pressures relative to the *Punti di Riconsegna* (PDR), and respective capacities. The focus of this study was on the total capacity of the network, with additional information available on the delivery point types, categorized by end-user applications such as distribution, industrial use, automotive, and thermoelectric.

To refine the dataset to the Sicilian context, particularly the provinces encompassing the network detailed in the previous section — Gela, Caltanissetta, Siracusa, Ragusa, and partially Enna and Messina — a targeted filtration process was implemented. The overarching objective was to attribute transport capacities and final gas usage types to each final node, as previously outlined.

Given the absence of precise coordinates directly associated with the delivery points, a reliance on geolocation was once again necessary. The assignment process prioritized proximity to cities, with nodes in close vicinity assigned the PDR dedicated to distribution, along with capacities deemed most plausible. Similarly, nodes proximate to industrial zones were assigned capacities reflective of industrial use, all while maintaining reference to the associated municipality. This geolocation approach was consistently applied across all end-use categories.

For the capacity and pressure assignment, only grade one nodes, i.e., entry or exit nodes from the network, were considered. It is important to specify that the pressure reported is the pressure relative to the pipeline to which the redelivery point is connected, as indicated by the TSO.

Regarding the portion of the network considered in this study, three entry points were identified and are summarized in table 3.3.

Entry points	Mass Flow [ $kg/s$ ]	Pressure [ $bar_g$ ]
Gela	346	75
Montalbano	1.5	75
Gagliano (Sparacollo)	1.5	75

**Table 3.3:** Entry points and mass flow

The flow rate entering the Gela entry point was read from official documents provided by the TSO [48].

On the other hand, with regard to the factual input nodes at Gagliano (Sparacollo) and Montalbano, it was decided to consider the flow demands of all the redelivery points in the Catania and Syracuse areas as assumptions of the flow rate subtracted from the National grid at these nodes. This summation was then divided between them and equally assigned.

The capacities, initially expressed within the database in  $[kWh]$  on a daily basis, have been converted to  $[kg/s]$ , leveraging the density and higher heating value of natural gas, parameters also sourced from Snam [49].

Considering [49]:

- Density  $\rho = 0.7836 \left[ \frac{kg}{sm^3} \right]$
- Higher Heating Value  $HHV = 0.039654 \left[ \frac{GJ}{sm^3} \right]$

As previously done, some of the exploited data are presented in table 3.4.

Node ID	Capacity $[kWh/d]$	Capacity $[kg/s]$	MOP $[bar_g]$
1	9269236	6.50	75
9	261579	0.18	75
12	722732	0.50	75
13	62977	0.04	75
15	302245	0.21	12
19	2129671	1.49	75
...	...	...	...
148	128337	0.09	24
149	235866	0.16	64
152	36996	0.03	12
153	1888203	1.32	12

**Table 3.4:** Delivery points capacity and pressure

This data preparation process ensured a realistic association of derived values with the final nodes, laying the foundation for subsequent simulations detailed in the following sections. This approach underscores the reliability of the simulated scenarios, enriching the analytical insights in this study.

### 3.3 SIMPLE algorithm and deblending model

In the following section a brief discussion of the fluid dynamic theory that feeds the SIMPLE model is addressed, followed by a description of the algorithm [50].

In addition, a brief explanation of how said algorithm is applied for the case study with a focus on deblending will be provided.

#### 3.3.1 Pressure Drop and Mass Equations

Given the pipe presented in figure 3.7, in order to derive the Pressure Drop Equation, it is useful to consider Newton's Second Law of Motion:

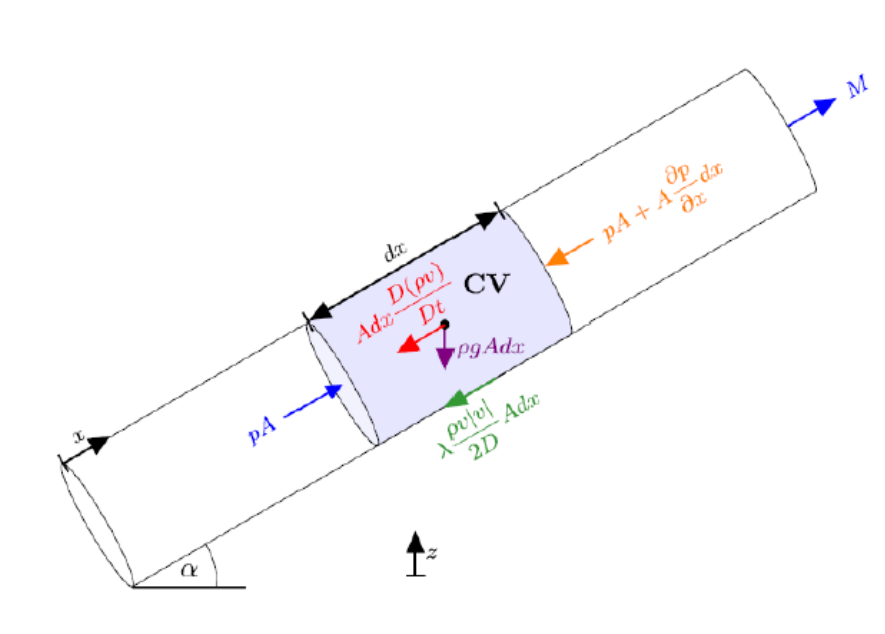


Figure 3.7: Schematized portion of a generic pipe

$$\frac{\partial(\rho v)}{\partial t} + \frac{\partial(\rho v^2)}{\partial x} + \frac{\partial p}{\partial x} + \frac{\lambda \rho v |v|}{2D} + \rho g \sin \alpha = 0 \quad (3.1)$$

By looking at equation 3.1, it is possible to recognize the following five different terms:

- $\frac{\partial(\rho v)}{\partial t}$  inertia term;
- $\frac{\partial(\rho v^2)}{\partial x}$  convective term;

- $\frac{\partial p}{\partial x}$  pressure force term;
- $\frac{\lambda \rho v |v|}{2D}$  shear force term;
- $\rho g \sin \alpha$  gravity force term.

Assuming the following hypothesis, it is possible to simplify equation 3.1:

- since the flow velocity in the pipes is  $v < 25 \text{ m/s}$ , it is possible to neglect the convective term, considering a creeping motion;
- since it is possible to assume slow changes at boundary conditions, it is possible to neglect the inertia term.

Thus obtaining equation 3.2

$$\frac{\partial p}{\partial x} + \frac{\lambda \rho v |v|}{2D} + \rho g \sin \alpha = 0 \quad (3.2)$$

Before proceeding, it could be interesting to show that the first of the aforementioned hypothesis is quite adequate for the problem; in fact:

$$\frac{\partial(\rho v^2)}{\partial x} + \frac{\partial p}{\partial x} = \frac{\partial}{\partial x} [p v^2 + p] = \frac{\partial}{\partial x} \left[ p \left( 1 + \frac{v^2}{c^2} \right) \right] \quad (3.3)$$

Assuming methane at the following conditions:

- $p = 5 \text{ bar}$
- $T = 15^\circ \text{C}$
- $c = 440 \text{ m/s}$
- $v = 25 \text{ m/s}$

$$\frac{\partial}{\partial x} \left[ p \left( 1 + \frac{v^2}{c^2} \right) \right] \sim \frac{\partial p}{\partial x} \quad (3.4)$$

In order to derive the Pressure Drop Equation, given the relationship 3.2 and the two hypotheses summarized before, it is possible to proceed towards the result simply substituting the definition of mass flow and introducing a new realistic hypothesis:

- isothermal flow, thus  $c^2 = \frac{p}{\rho}$

Thus obtaining:

$$\frac{dp}{dx} + \frac{p}{c^2} g \sin \alpha = -\lambda c^2 \frac{\dot{m} |\dot{m}|}{\rho A^2 2D} \quad (3.5)$$

Finally, introducing the quantity  $P = p^2$ , it is possible to derive the generic Pressure Drop Equation for a pipe, known also as the Fregusson Equation:

$$\frac{dP}{dx} + \frac{2g \sin \alpha}{c^2} P = -\lambda c^2 \frac{\dot{m} |\dot{m}|}{A^2 D} \quad (3.6)$$

Performing the integration along the pipeline length  $L$ :

$$P_1 - P_2 e^s = \frac{\lambda c^2 l_e}{A^2 D} \dot{m} |\dot{m}| \quad (3.7)$$

Where:

- $s = \frac{2g(H_2 - H_1)}{c^2}$
- $l_e = \begin{cases} \frac{e^s - 1}{s} l & H_2 \neq H_1 \\ l & H_2 = H_1 \end{cases}$

Equation 3.7 can be further simplified considering horizontal pipes and referring to the volumetric flow  $Q$  [ $S m^3/h$ ] as follows:

$$p_{in}^2 - p_{out}^2 = R_f |Q| Q \quad (3.8)$$

Where  $R_f = \frac{16 \lambda \rho_n^2 c^2 l}{\pi^2 D^5}$

$\lambda$  is called friction factor and depends on the Reynolds number which characterize the flow.

$$Re = \frac{\rho v D}{\mu} \quad (3.9)$$

In case of laminar flow:

$$\lambda = \frac{Re}{64} \quad (3.10)$$

In case of turbulent flow, the implicit relationship between  $\lambda$  and  $Re$  is given by the Colebrook White equation:

$$\frac{1}{\sqrt{\lambda}} = -2 \log_{10} \left( \frac{2.51}{Re \sqrt{\lambda}} + \frac{3}{3.71 D} \right) \quad (3.11)$$

Since  $r$  is the internal pipeline roughness, the correlation between the friction factor and the Reynolds number can also be derived from the Moody Diagram presented in figure 3.8.

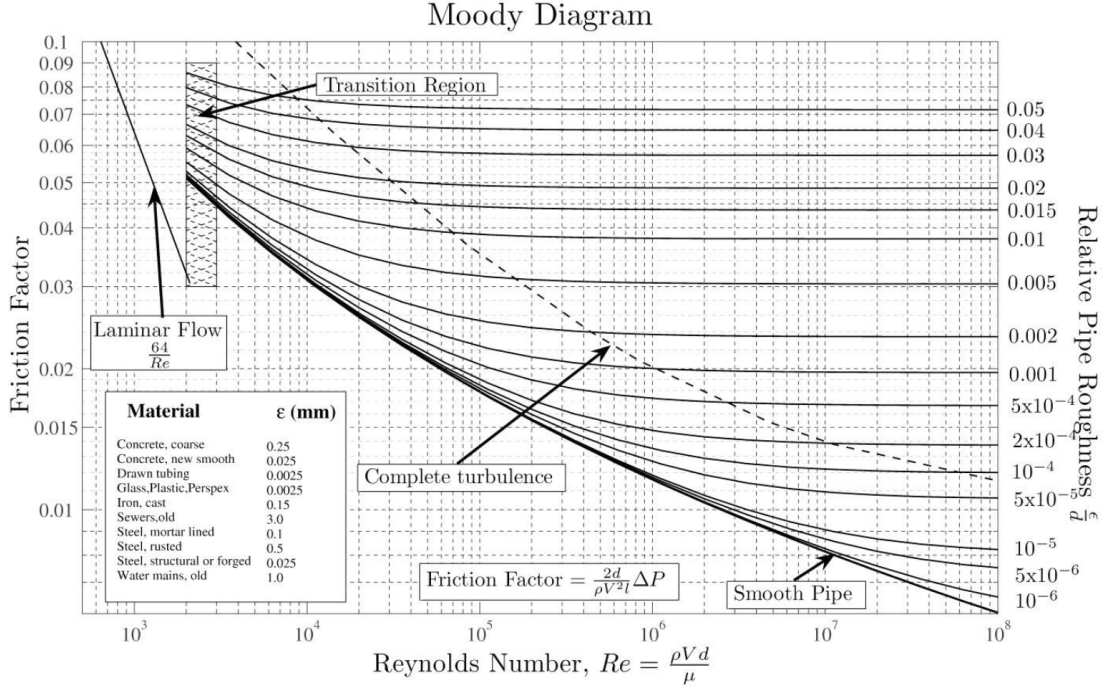


**Figure 3.8:** Moody Diagram [51]

In order to proceed towards the *SIMPLE* algorithm, adjusted for gas networks, it is useful to make some considerations about the conservation of mass, or state equation. Given all the previous hypothesis, the state equation can be written as follows:

$$\frac{\partial(\rho v)}{\partial x} = 0 \quad (3.12)$$

For a compressible flow, where  $\rho = f(T, p)$ :

$$\frac{\partial(\rho v)}{\partial x} = \frac{\partial}{\partial x} \left( \frac{\dot{m}}{A} \right) = \frac{1}{A} \frac{\partial \dot{m}}{\partial x} = 0 \quad (3.13)$$

Hence,

$$XM + M_{ext} = 0 \quad (3.14)$$

In conclusion, considering both the previous explained mass conservation equation, and the rewritten Newton's law of equation 3.2 in case of horizontal pipes, the two equations that feed the *SIMPLE* algorithm, adjusted for gas networks, are

summarized in the following:

$$\begin{cases} \frac{1}{A} \frac{\partial \dot{m}}{\partial x} = 0 \\ p_{in}^2 - p_{out}^2 = R_{fc}(\dot{m}) \dot{m} \end{cases} \quad (3.15)$$

The previous equations can also be rewritten in a more convenient way for automated calculation:

$$\begin{cases} XM + M_{ext} = 0 \\ X^t \mathcal{P} = R_{fc}(M) M \end{cases} \quad (3.16)$$

Keeping in mind that:

$$\begin{cases} \mathcal{P} = P^2 \\ R_{fc} = \frac{\lambda c^2 L}{A^2 D} |\dot{m}| \end{cases} \quad (3.17)$$

### 3.3.2 *SIMPLE* Algorithm

The *SIMPLE* Algorithm (Semi-Implicit Method for Pressure-Linked Equations) is an iterative procedure that allows the user to solve the coupled Navier-Stokes equations presented before.

It is important to observe that the continuity equation conceals a system of  $n$  equations with  $b$  unknowns, while the momentum conservation equation is a system of  $b$  equations with  $n$  unknowns. Hence, the system of size  $n+b$  exactly encompasses  $b+n$  unknowns, allowing for the potential of a unique solution. From the previous presented equations:

$$\begin{cases} XM + M_{ext} = 0 \\ X^t \mathcal{P} = R_{fc}(M) M \end{cases} \quad (3.18)$$

It is possible to rewrite the momentum law in a nearly explicit form for the mass flow rate as follows:

$$\begin{cases} XM + M_{ext} = 0 \\ M = Y_{fc} \mathcal{P} X^t \end{cases} \quad (3.19)$$

Knowing that:

$$Y_{fc} = inv(R_{fc}(M)) = \begin{bmatrix} 1/R_c & 0 & 0 \\ 0 & 1/R_c & 0 \\ 0 & 0 & 1/R_c \end{bmatrix} \quad (3.20)$$

The two critical features of this mathematical problem are given by the fact that firstly, the momentum equation cannot be directly solved since there is a hidden dependence due to the advective term, and secondly, the mass flow rate, appearing in both the equations, couples the problem, forcing the two equations to be solved simultaneously.

The model proposed in the following, invented by *Panktar et Spalding* in 1972 and then adapted to networks of compressible fluids, provides a robust approach for solving this problem. The algorithm can easily be explained following four different steps, after an initial definition.

- Definition - given the exact solution  $M$ , it can be written as the sum of a guessed solution  $M^*$  plus a correction  $M'$ , obtaining:

$$M = M^* + M' \quad \mathcal{P} = \mathcal{P}^* + \mathcal{P}' \quad (3.21)$$

- Step 1: subtraction between the true momentum equation and the guessed momentum equation:

$$\begin{aligned} M &= Y_{f_c} X^t \mathcal{P} - \\ M^* &= Y_{f_c}^* X^t \mathcal{P}^* = \\ &\dots \\ M - M^* &= Y_{f_c} X^t \mathcal{P} - Y_{f_c}^* X^t \mathcal{P}^* \end{aligned}$$

- Step 2: assumption of weak non linearity. If the non linearity is assumed to be weak, it is possible to write that  $Y_{f_c}(M) = Y_{f_c}^*(M^*)$ , thus obtaining one equation relating the mass flow rate corrections  $M'$  to the pressure corrections  $\mathcal{P}'$ , known as the Mass Flow Rate Correction Equation:

$$\begin{aligned} M - M^* &= Y_{f_c} X^t (\mathcal{P} - \mathcal{P}^*) \\ M' &= Y_{f_c} X^t \mathcal{P}' \end{aligned} \quad (3.22)$$

- Step 3: writing the continuity equation with guessed-correction decomposition, keeping in mind that  $Y_{f_c}(M) = Y_{f_c}^*(M^*)$ :

$$X M^* + X M' + M_{ext} = 0 \quad (3.23)$$

- Step 4: substitution of the mass flow rate correction of step 2 into the equation obtained from step 3, thus obtaining an equation for the pressure correction  $\mathcal{P}'$ :

$$X Y_{f_c} X^t \mathcal{P}' = -X M^* - M_{ext} \quad (3.24)$$

$$H \mathcal{P}' = b \quad (3.25)$$

$$\mathcal{P}' = H \setminus b \quad (3.26)$$

Finally, it is possible to apply the calculated corrections and iterate the process until a convergence criteria is satisfied.

$$\mathcal{P}^{*new} = \mathcal{P}^* + \mathcal{P}' \quad (3.27)$$

$$M^{*new} = M^* + M' \quad (3.28)$$

Until

$$\mathcal{P}^{*new} = \mathcal{P}^* \quad (3.29)$$

$$M^{*new} = M^* \quad (3.30)$$

In order to dampen the magnitude of the corrections and help the algorithm to move towards the convergence, it is also possible to introduce two over-relaxation factors for the *SIMPLE* method:

$$\alpha_p = [0 \div 1]$$

$$\alpha_M = [0 \div 1]$$

These two factors are used when the corrections are applied:

$$\mathcal{P}^{*new} = \mathcal{P}^* + \alpha_p \mathcal{P}' \quad (3.31)$$

$$M^{*new} = M^* + \alpha_M M' \quad (3.32)$$

### 3.4 Deblending model

By integrating the SIMPLE algorithm into the deblending model, the MATLAB code ensures a systematic and iterative approach to adjusting the gas mixture properties, accounting for changes in composition, mass fractions, and pressure fields. The iterative nature of SIMPLE allows for an accurate representation of the dynamic behavior of the gas mixture during the deblending processes.

The deblending algorithm encompasses several essential steps aimed at refining the composition of hydrogen and methane at specific nodes, alongside the adjustment of external gas flow conditions.

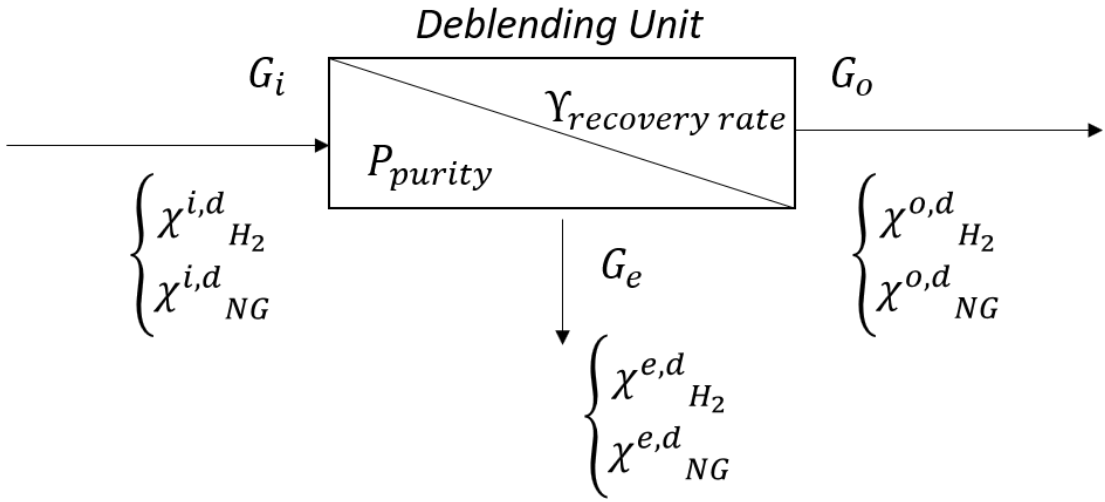


**Figure 3.9:** Scheme of the deblending unit represented as a black box

With reference to the scheme of the deblending unit presented as a black box in figure 3.9, the following notation is considered:

- $d$ : deblending unit
- $i$ : input
- $o$ : output
- $e$ : extracted
- $G$ : mass flow
- $\Upsilon$ : recovery rate  $\Upsilon = \frac{1 - \chi_{H_2}^{o,d}}{\chi_{H_2}^{i,d}}$

- $\chi$ : molar fraction
- $P$ : purity, or the molar fraction of the hydrogen in the extraction stream

From the application of the mass conservation equation for each of the chemical species, equations 3.33 and 3.34 were derived:

$$\begin{cases} \chi_{H_2}^{e,d} = P \\ \chi_{NG}^{e,d} = 1 - \chi_{H_2}^{e,d} = 1 - P \end{cases} \quad (3.33)$$

$$\begin{cases} \chi_{H_2}^{o,d} = \frac{\chi_{H_2}^{i,d} (1 - \Upsilon)}{\chi_{H_2}^{i,d} (1 - \Upsilon) + (1 - \chi_{H_2}^{i,d}) - \chi_{H_2}^{i,d} \Upsilon \left(\frac{1-P}{P}\right)} \\ \chi_{NG}^{o,d} = 1 - \chi_{H_2}^{o,d} \end{cases} \quad (3.34)$$

The boundary condition which satisfies the thermal demand from the final user is imposed at the exit of the debinding unit. Considering  $E_{th,req}$  as the thermal energy request:

$$G_o = \frac{E_{th,req}}{HHV} \quad (3.35)$$

It is important to note that, using this equation, the gas flow rate out of the debinding unit is set as a function of the unit's output composition.

As for the flow demand upstream of the debinding unit, this is calculated by applying the conservation of mass of the debinding unit itself:

$$\begin{aligned} G_o &= G_i - G_e = \\ &= G_i - \left[ G_i \Upsilon \chi_{H_2}^{i,d} + G_i \Upsilon \chi_{H_2}^{i,d} \left(\frac{1-P}{P}\right) \right] = \\ &= G_i \left[ 1 - \left[ \Upsilon \chi_{H_2}^{i,d} + \Upsilon \chi_{H_2}^{i,d} \left(\frac{1-P}{P}\right) \right] \right] = \\ &= G_i \left[ 1 - \left[ \Upsilon \chi_{H_2}^{i,d} \left(1 + \frac{1-P}{P}\right) \right] \right] = \\ &= G_i \left[ 1 - \frac{\Upsilon \chi_{H_2}^{i,d}}{P} \right] \end{aligned}$$

Hence:

$$G_i = \frac{G_o}{1 - \frac{\Upsilon \chi_{H_2}^{i,d}}{P}} \quad (3.36)$$

$$G_e = \frac{G_i \Upsilon \chi_{H_2}^{i,d}}{P} \quad (3.37)$$

Where  $G_e$  is the mass flow extracted and re-injected at the previous node.

# Chapter 4

## Simulations and results

This section outlines the simulation outcomes of integrating hydrogen into the natural gas network in Southern Sicily.

The behavior of gas mixtures at delivery points and the gradual re-injection of separated hydrogen has been examined for each blending scenario, with the objective of finding out the  $H_2$  concentrations obtained in correspondence with the industrial area of the Syracuse Petrochemical Hub.

### 4.1 Simulation settings

In accordance with the Transmission System Operator's transport capacity database, four distinct types of redelivery points exist, categorized by the final user types: industrial, automotive, distribution, and thermoelectric sectors.

Based on the locations of the final nodes identified in section 3.2.1, each has been assigned a specific user type. Subsequently, after assigning user types, and drawing from the debinding information provided in the section 2.4, recovery rates and purity levels of the extracted hydrogen were allocated to each user. These details are summarized in table 4.1.

Final User	Recovery Rate	Purity
Industrial	0.9	0.997
Automotive	0.9	0.980
Distribution	0.9	0.997
Thermoelectric	0.9	0.997

**Table 4.1:** Recovery Rate and Purity for each final user typology

All final nodes, except for the entry nodes identified in section 3.2.1, underwent the deblending process.

An exception was made for the ones located at the Syracuse Petrochemical Hub, where only hydrogen extraction was planned, avoiding the reinjection process.

Values were saved to assess the extractable hydrogen quantity after accumulation in the network.

The simulations presented in this section are conducted using the MATLAB model based on the SIMPLE algorithm, covered in section 3.3.

In this model, the coordinates of the final nodes are maintained and reproduced, enhancing the clarity of the obtained results. Figure 4.1 serves as an illustrative example, portraying the network without specific information on flow rates and pressures.

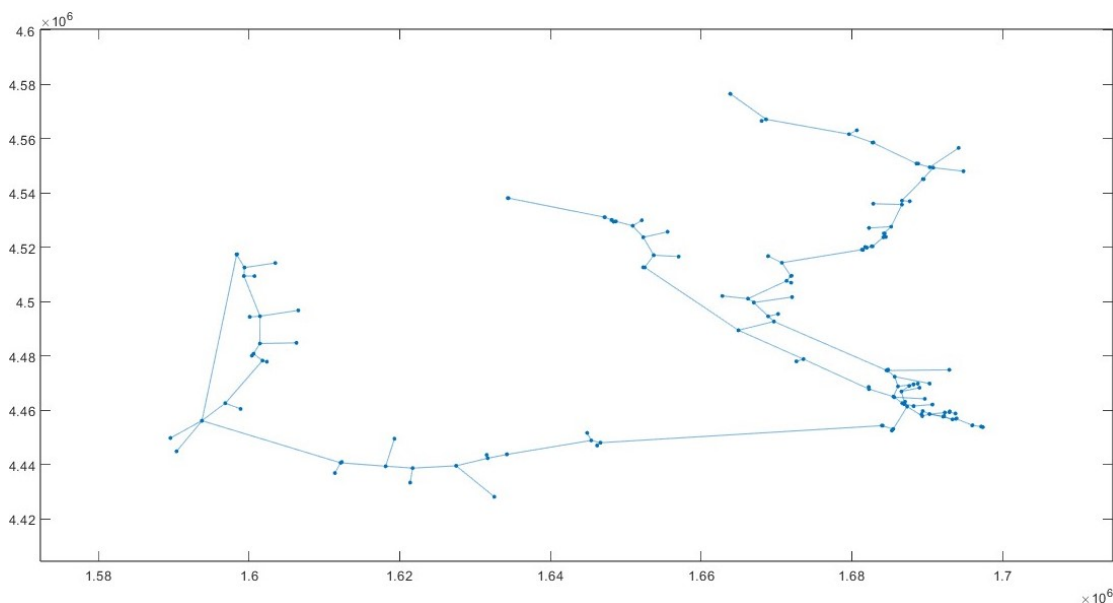


**Figure 4.1:** Network model on MATLAB, considering coordinates

In the following subsections, four distinct simulation scenarios will be explored: the base case, where the network is hydrogen-free, a scenario incorporating a 5% hydrogen blend, another with a 10% blend, and a final case with a more substantial 20% hydrogen blend.

This structured approach allows for a comprehensive examination of the network under varying hydrogen concentrations, providing insights into its dynamic behavior and performance.

## 4.2 Base case: no hydrogen blending

The main purpose of this simulation is to establish a baseline for subsequent simulations, considering a network exclusively flowed through by methane without the addition of hydrogen.

Flow values from section 3.2.2, along with pressure values at entry points—especially at the national entry point in Gela—have been integrated.

Using the previously described algorithm, the network was graphically represented with visual indications of gas quantity, proportionate to symbol size in Figure 4.2, and nodal pressure.

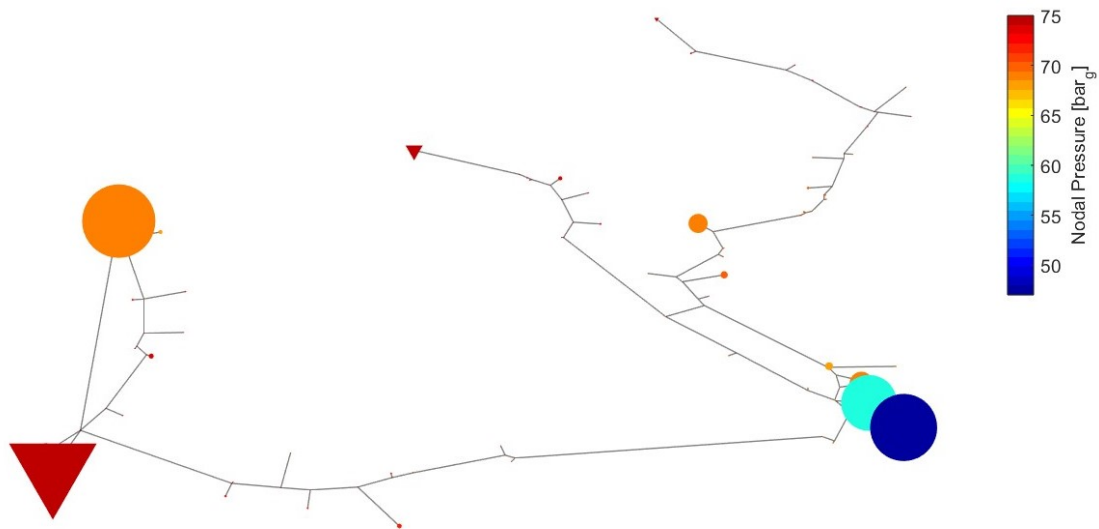


**Figure 4.2:** Nodal pressures and flow rates

Significant flows are observed at the National entry point in Gela, the interconnection node in Enna, and near the Syracuse Petrochemical Hub, while smaller symbols, representing predominantly distribution points, indicate lower demand. The node near Gagliano is confirmed as an entry point, receiving gas from the national network. Conversely, the node near Montalbano, initially assumed as an entry point, is reevaluated as an exit node.

Regarding pressures, entry points exhibit intense red corresponding to the initially set 75 bar<sub>g</sub> pressure. Moving away from entry points reveals significant pressure drops, reaching below 50 bar<sub>g</sub>.

In Figure 4.3, a focus on flows at network boundaries highlights that, despite efforts to consider all demands in the area, these remain comparatively small compared to incoming gas in Sicily, industrial zone demands, and gas allocated for transportation in the broader region or Italy.

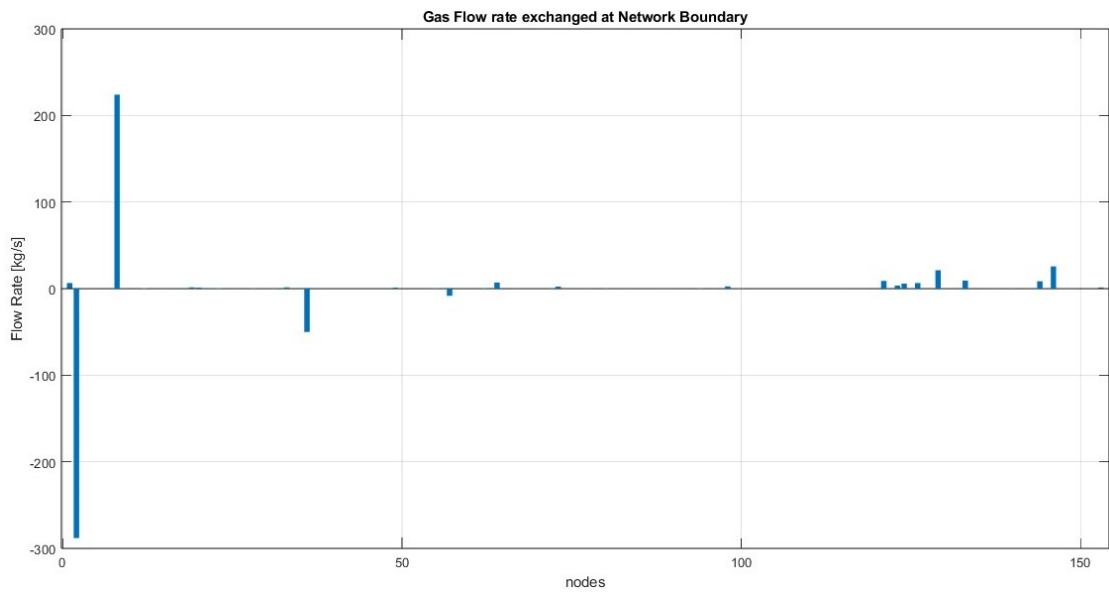


**Figure 4.3:** Gas flow rates at network boundaries

Figure 4.4 underscores examples where, given the assigned demands at final nodes, the initially assumed gas flow direction in certain network sections deviates from actual network needs. Negative flows represent corrections derived from the simulation.

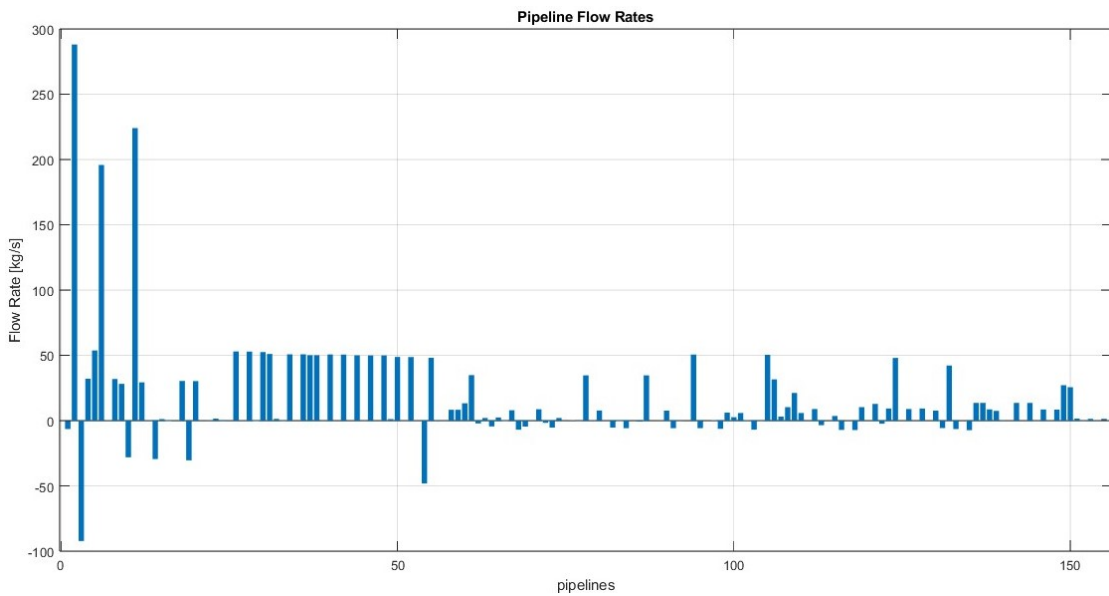


**Figure 4.4:** Pipeline flow rates

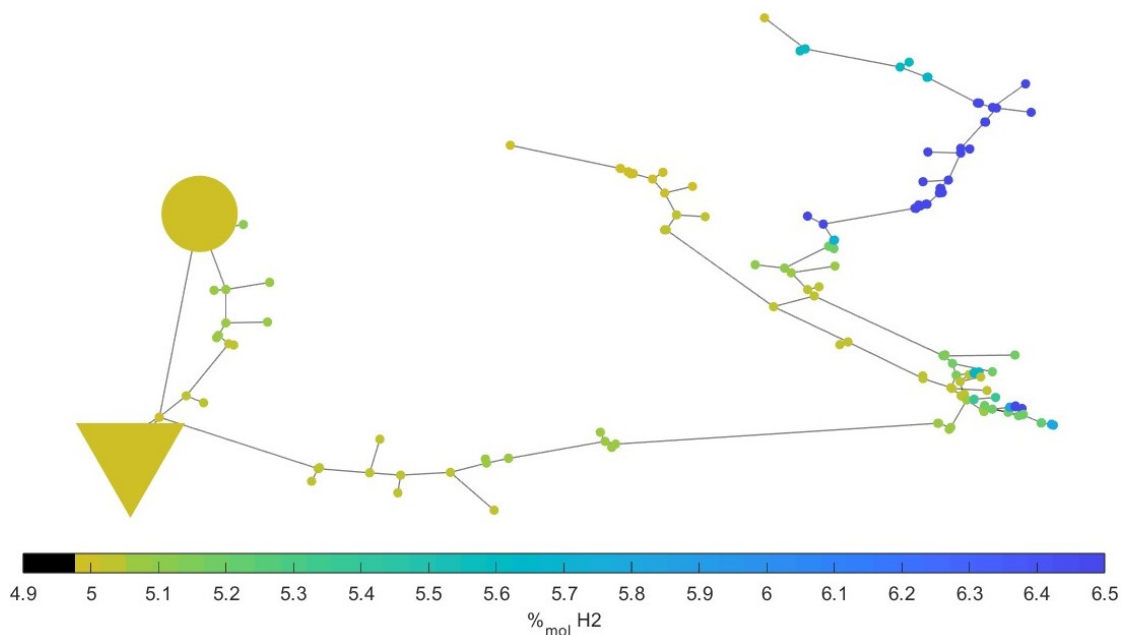
### 4.3 5% Hydrogen blending

This paragraph outlines the simulation involving a 5% hydrogen blend in the gas network.

The simulations conducted primarily focused on hydrogen accumulation throughout the network and the extraction of hydrogen in the more industrialized zone. To emphasize the impact of extraction on hydrogen distribution, the simulations took a dual approach. Firstly, a simulation was executed without extraction, solely observing the accumulation and propagation of hydrogen in the network. Subsequently, extraction was applied. The results of these two scenarios are compared in the following figures.

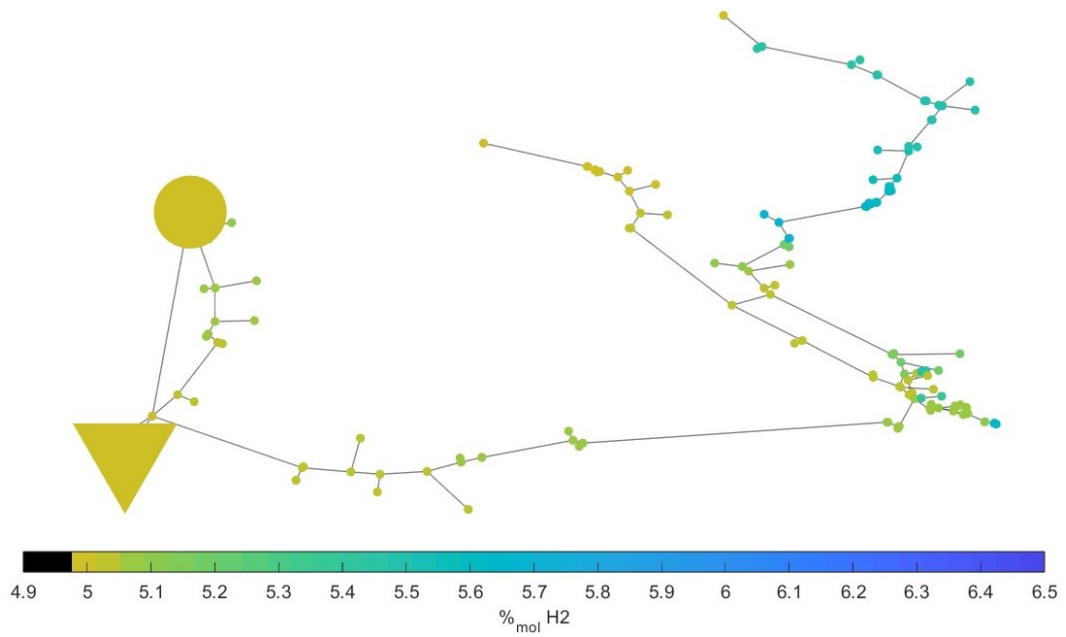
Figures 4.5 and 4.6 depict the hydrogen share in the network for the case with and without hydrogen extraction.

Although the left portion of both networks is nearly identical, notable differences emerge in the region where extraction occurs on the right.



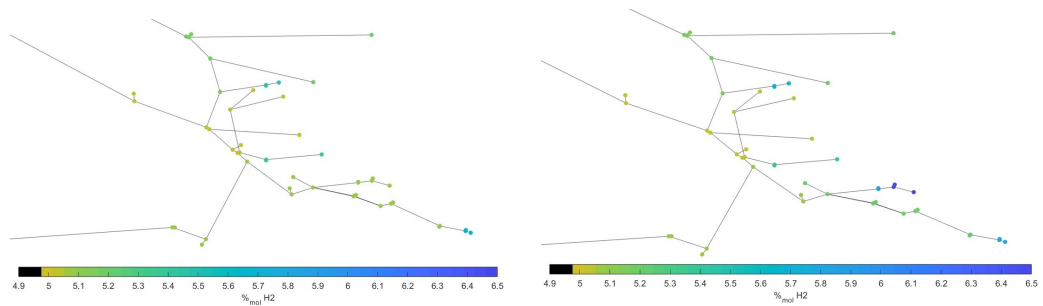
**Figure 4.5:** Hydrogen distribution through the network without  $H_2$  extraction - 5% blend case

In the first scenario, the absence of hydrogen extraction at the petrochemical complex leads to concentrations exceeding 6.5% both in the affected area and downstream in the network. Hydrogen extraction, guided by the previously set separation yields and purities, keeps the hydrogen concentration in the network constrained to values below 6%.



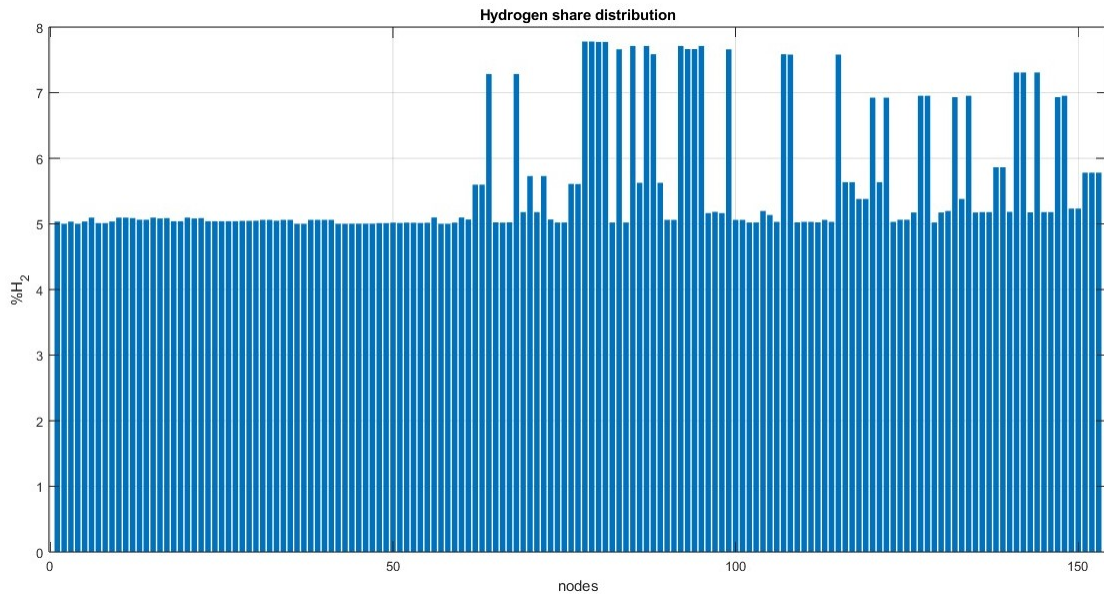
**Figure 4.6:** Hydrogen distribution through the network with  $H_2$  extraction - 5% blend case

Figure 4.7 shows a close-up of the area targeted by the extraction process to highlight the differences in the molar concentrations of hydrogen in the nodes before and after extraction.



**Figure 4.7:** Comparison of hydrogen extraction area - with and without  $H_2$  extraction

Figures 4.8 and 4.9 offer a detailed depiction of hydrogen distribution across all 153 nodes in the network.



**Figure 4.8:**  $H_2$  share distribution without extraction - 5% blend case

These graphs make it easier to observe the impact of extraction and how this effect extends to nodes in the western zone, beyond the industrial area, where initial hydrogen concentrations were elevated.

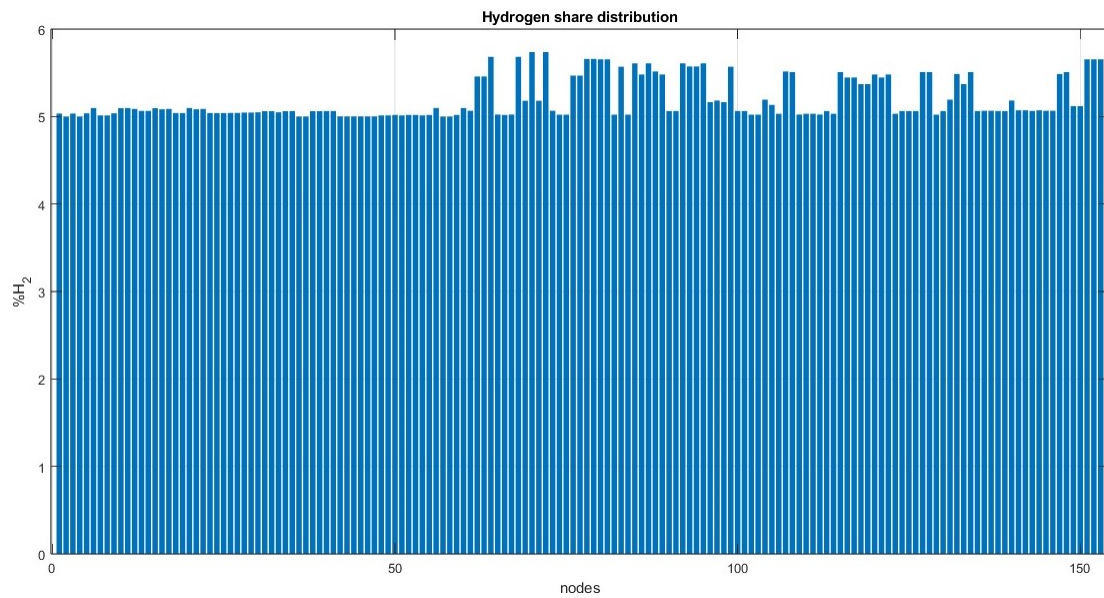


**Figure 4.9:**  $H_2$  share distribution with extraction - 5% blend case

Table 4.2 provides the extracted hydrogen flows at the dedicated extraction nodes:

Nodes ID	$H_2$ extracted [kg/h]
114	$1.837 \cdot 10^4$
117	$2.014 \cdot 10^4$
121	$2.284 \cdot 10^{-1}$
123	8.324
129	$5.038 \cdot 10^{-1}$
131	$1.402 \cdot 10^2$
133	$2.356 \cdot 10^{-1}$
137	$2.659 \cdot 10^2$
144	$2.023 \cdot 10^{-1}$
146	$6.132 \cdot 10^{-1}$

**Table 4.2:** Mass flow rate of extracted hydrogen - 5% blend case

The total flow rate of extracted hydrogen from the industrial nodes in the Syracuse Petrochemical Hub is:

$$Total H_2 Extraction = 186.7 \text{ kg/h} \tag{4.1}$$

## 4.4 10% Hydrogen blending

This paragraph addresses the scenario with a gas blend of 10% hydrogen in the network. The simulations, in this case as well, focused on hydrogen accumulation throughout the network and the extraction of hydrogen in the more industrialized zone.

Unlike the previous analysis, the scenario without extraction was not considered, as the previous analysis indicated a clear increase in concentration in the absence of hydrogen utilization along the network. It is, however, significant to observe the hydrogen concentrations reached in nodes identified as most sensitive during the analysis as seen in 4.10.

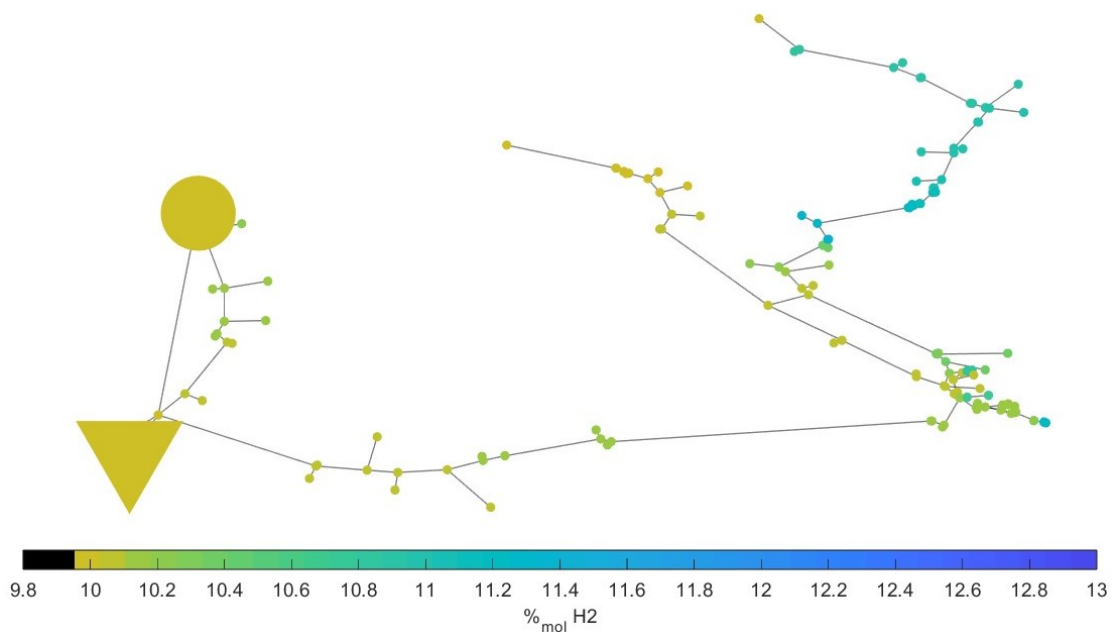


**Figure 4.10:** Hydrogen distribution through the network with extraction - 10% blend case

In this instance, as observed in figure 4.11, the concentrations achieved surpass the initial hydrogen concentration in the network by more than one percentage point, even considering a hydrogen extraction rate of the selected nodes.

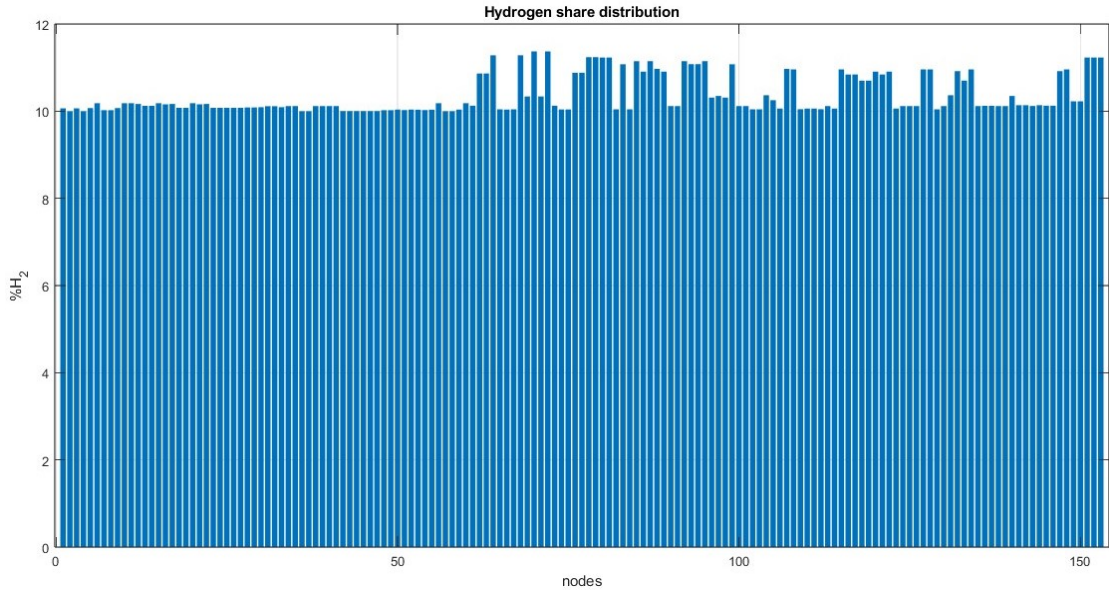


**Figure 4.11:**  $H_2$  share distribution with extraction - 10% blend case

Table 4.3 provides the extracted hydrogen flows at the dedicated extraction nodes:

Nodes ID	$H_2$ extracted [kg/s]
114	$3.849 \cdot 10^{-4}$
117	$4.217 \cdot 10^{-4}$
121	$4.783 \cdot 10^{-4}$
123	$1.744 \cdot 10^{-4}$
129	$1.055 \cdot 10^{-2}$
131	$2.937 \cdot 10^{-2}$
133	$4.934 \cdot 10^{-2}$
137	$5.570 \cdot 10^{-2}$
144	$4.238 \cdot 10^{-2}$
146	$1.285 \cdot 10^{-2}$

**Table 4.3:** Mass flow rate of extracted hydrogen - 10% blend case

The total flow rate of extracted hydrogen from the industrial nodes in the Syracuse Petrochemical Hub is:

$$Total H_2 Extraction = 391.1 \text{ kg/h} \quad (4.2)$$

## 4.5 20% Hydrogen blending

For the final simulation, a scenario with a network mixture characterized by a 20% hydrogen blend was considered. Similar to the previous case, the focus was on hydrogen accumulation throughout the network and hydrogen extraction in the petrochemical complex area.

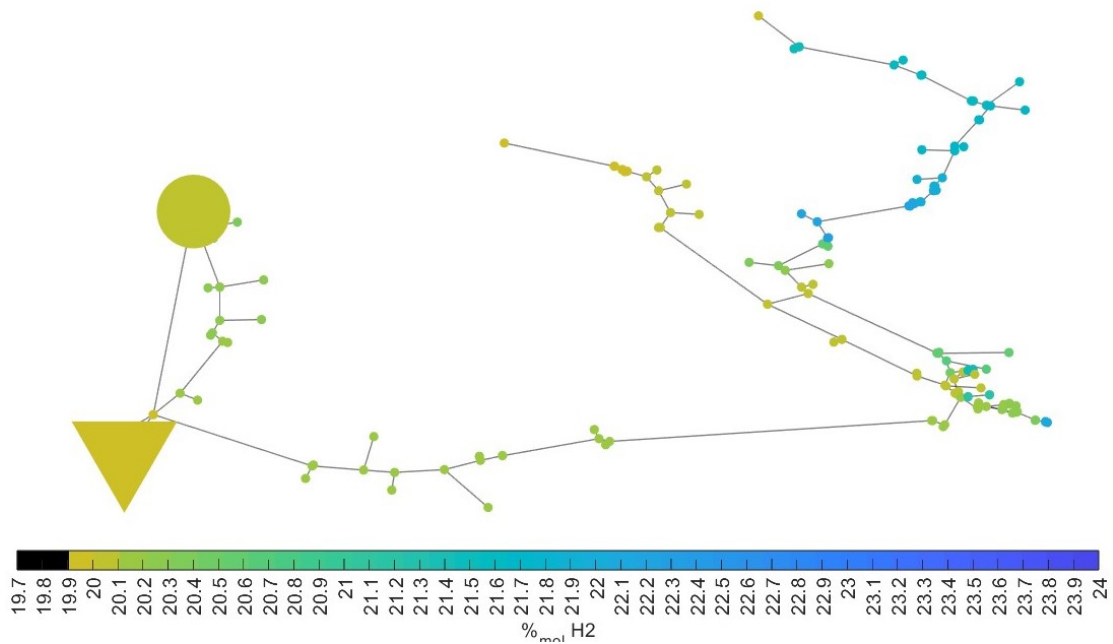


**Figure 4.12:** Hydrogen distribution through the network with extraction - 20% blend case

As in the previous scenario, we observed the varied hydrogen concentrations achieved at the key nodes of our study and those downstream. In figure 4.13, it can be noted that the remaining hydrogen percentage in the network, even after extraction, reaches almost 3% more than the initial concentration at some points, indicating significant accumulation in the network despite the extracted hydrogen.

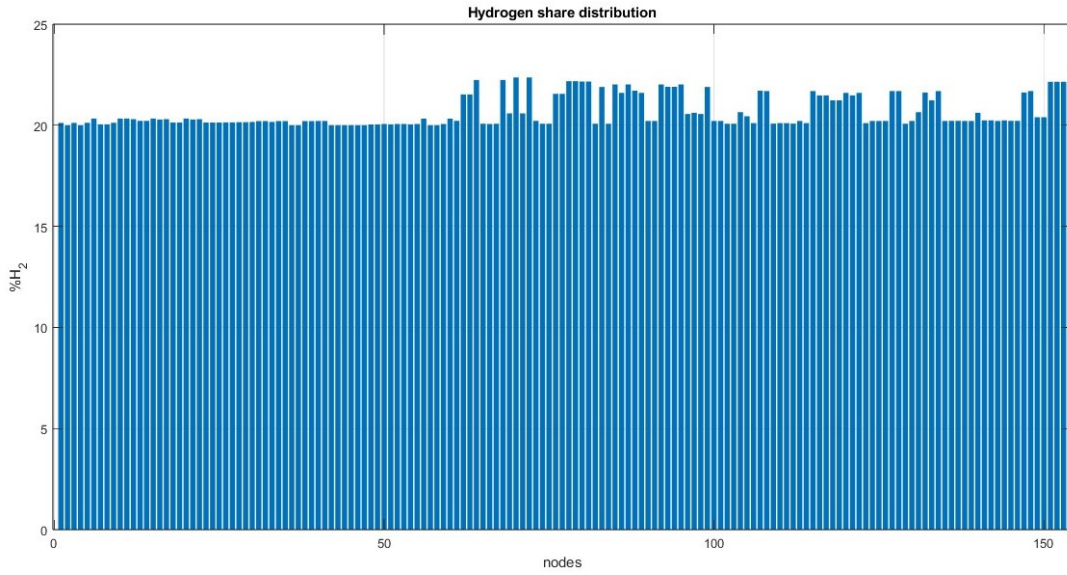


**Figure 4.13:**  $H_2$  share distribution with extraction - 20% blend case

Table 4.4 provides the extracted hydrogen flows at dedicated extraction nodes:

Nodes ID	$H_2$ extracted [kg/h]
114	$8.51 \cdot 10^{-4}$
117	$9.30 \cdot 10^{-4}$
121	$1.06 \cdot 10^2$
123	$3.85 \cdot 10$
129	$2.33 \cdot 10^2$
131	$6.49 \cdot 10^{-2}$
133	$1.09 \cdot 10^2$
137	$1.23 \cdot 10^{-1}$
144	$9.36 \cdot 10$
146	$2.84 \cdot 10^2$

**Table 4.4:** Mass flow rate of extracted hydrogen - 20% blend case

The total flow rate of extracted hydrogen from the selected industrial nodes in the Southeast Sicily area is:

$$Total H_2 Extraction = 864.0 \text{ kg/h} \quad (4.3)$$

# Chapter 5

## Discussion of results and conclusions

In the previous chapter, the results of the investigation of hydrogen deblending into a part of the Sicilian transmission network have been presented.

This chapter focuses on a broader discussion of the findings, aiming to unveil their significance and contributions to the hydrogen integration into the gas infrastructure field. Key patterns and any possible anomalies will be explored through a critical analysis of the data and methodology in order to identify any potential findings and useful insights for possible developments on the topic.

### 5.1 Discussion of results

The initial focus of our investigation centers on the quality of the gas mixture, specifically on examining the variations in relative density, higher heating value, and Wobbe index as the concentrations of hydrogen within the mixture change. The purpose of this analysis is to ensure that, in light of the simulation results concerning hydrogen accumulation in the network discussed in preceding sections, the three aforementioned parameters conform to the prescribed intervals outlined in the ministerial decree dated May 18th, 2018 [52]. The decree establishes technical guidelines governing the chemical-physical characteristics and the presence of additional components in combustible gas to be piped.

The acceptable ranges for these parameters are detailed in table 5.1.

Parameter	Interval	Unit
Higher Heating Value	34.95 - 45.28	$MJ/Sm^3$
Wobbe Index	47.31 - 52.33	$MJ/Sm^3$
Relative density	0.555 - 0.7	

**Table 5.1:** Allowable ranges of the  $HHV$ ,  $WI$  and  $\rho$  in Italy [52]

In order to conduct these analyses, values of the density and higher heating value of both natural gas [53] and hydrogen [54] were sourced along with air density, with reference to standard conditions. Natural gas properties refer to the Libyan gas entering Italy through the Gela terminal via the Greenstream pipeline.

Gas density values are presented in tables 5.2:

$\rho_{air}$ [ $kg/Smc$ ]	$\rho_{H_2}$ [ $kg/Smc$ ]	$\rho_{NG}$ [ $kg/Smc$ ]
1.225	0.0852	0.7836

**Table 5.2:** Air, Hydrogen and natural gas densities in standard conditions

Gas higher heating values for hydrogen and natural gas are presented in table 5.3.

$HHV_{H_2}$ [ $MJ/Smc$ ]	$HHV_{NG}$ [ $MJ/Smc$ ]
12.70	39.65

**Table 5.3:** Hydrogen and natural gas higher heating values in standard conditions

Subsequently, the values of  $HHV$  and density of the mixture were computed, factoring in the molar fraction of hydrogen and natural gas in the blend, according to the following formulas:

$$HHV_{mix} = HHV_{NG} \cdot \chi_{NG} + HHV_{H_2} \cdot \chi_{H_2} \quad (5.1)$$

$$\rho_{mix} = \rho_{NG} \cdot \chi_{NG} + \rho_{H_2} \cdot \chi_{H_2} \quad (5.2)$$

The values of  $HHV_{mix}$  and  $\rho_{mix}$  calculated using the aforementioned formulas will be instrumental in determining the relative density and Wobbe index, as defined below:

$$\rho_{rel} = \frac{\rho_{mix}}{\rho_{air}} \quad (5.3)$$

$$WI = \frac{HHV}{\sqrt{\rho}} \quad (5.4)$$

By doing so, the gas quality values obtained for different concentrations of hydrogen in the mixture are computed and summarized in table 5.4.

% $H_2$	% NG	$HHV_{mix}$ [MJ/Sm <sup>3</sup> ]	WI [MJ/Sm <sup>3</sup> ]	$\rho_{rel}$
0%	100%	39.65	49.58	0.6397
5%	95%	38.30	48.99	0.6112
10%	90%	36.96	48.41	0.5827
15%	85%	35.60	47.83	0.5542
20%	80%	34.26	47.25	0.5257
30%	70%	31.57	46.11	0.4686

**Table 5.4:** Gas quality variations with %  $H_2$

The obtained values have been graphically depicted alongside the lower limit ranges presented in table 5.1 to visually illustrate the percentage of hydrogen in the mixture that causes the gas quality parameters to fall outside the acceptable limits.

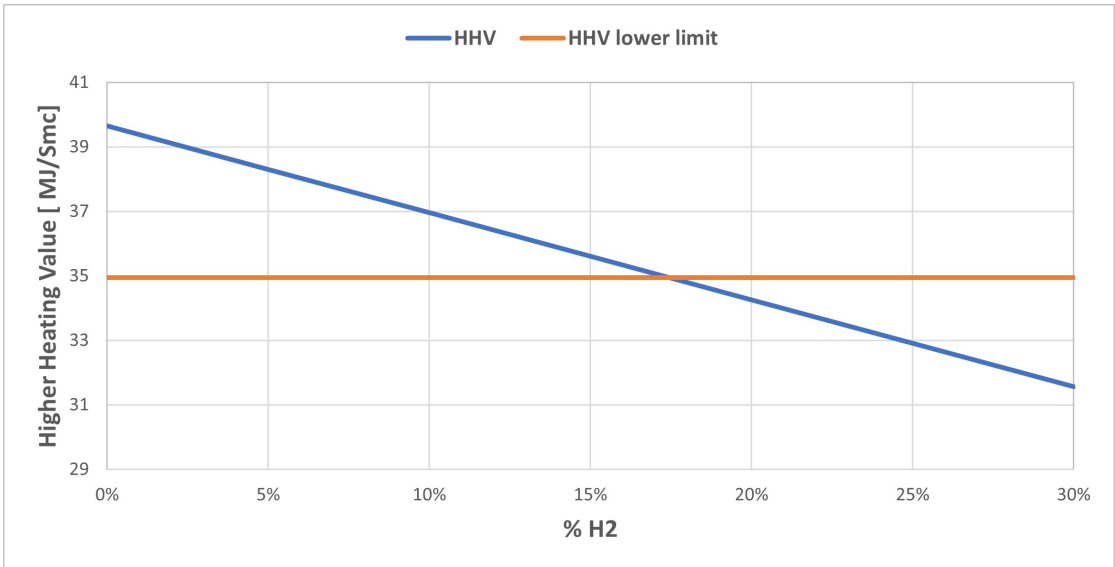


**Figure 5.1:** Higher Heating Value trend based on percentage of  $H_2$  in the mixture

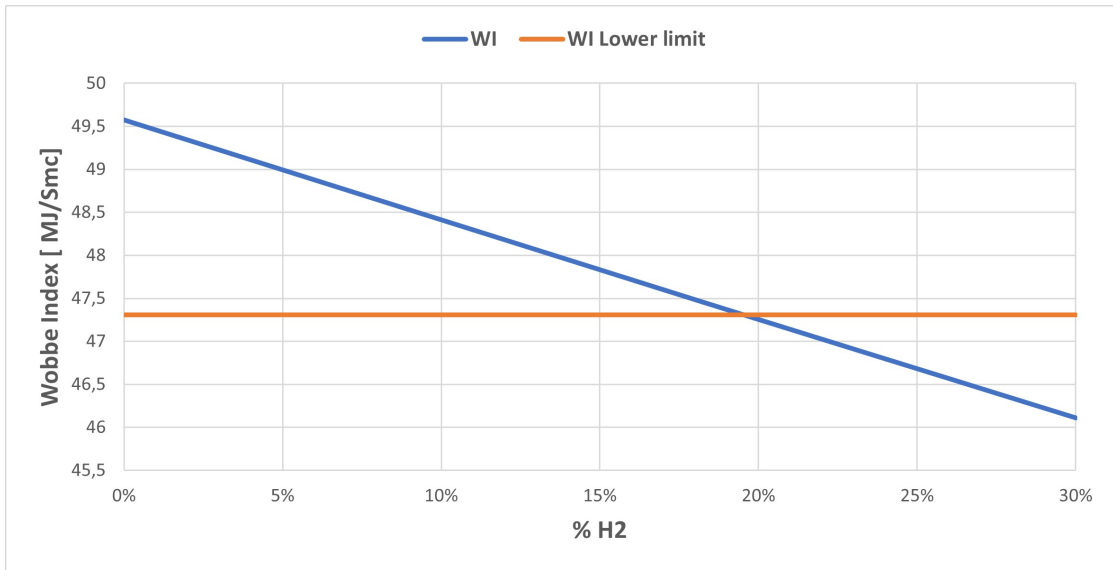


**Figure 5.2:** Wobbe Index trend based on percentage of  $H_2$  in the mixture

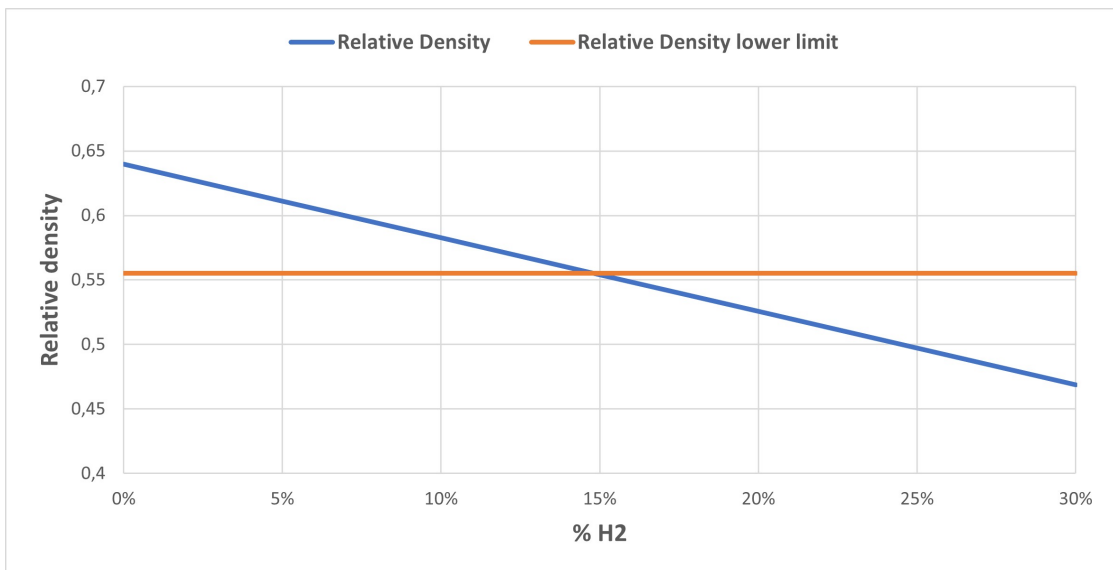


**Figure 5.3:** Relative density trend based on percentage of  $H_2$  in the mixture

The obtained graphs reveal that acceptability limits vary depending on the considered parameter, with relative density as the limiting factor. The minimum acceptable value of hydrogen share, as observed in Table 5.5, is 14.9%.

This implies that, among the considered scenarios in this simulation, given the nodal hydrogen percentages obtained in the previous section, a blend with 20%

Parameter	$H_2$ share
Higher Heating Value	17.5 %
Wobbe Index	19.6 %
Relative density	14.9 %

**Table 5.5:** Hydrogen share acceptability limit

hydrogen would not be permissible according to current directives. This is in contrast to cases with 5% and 10% blends, which meet the acceptability criteria.

However, while relative density emerges as the most limiting factor, from the preceding graphs it is evident that a 20% hydrogen concentration would not be acceptable even concerning higher heating value and Wobbe index intervals, both falling below the 20% threshold.

It is important to note that, although the analyses have been conducted for various concentrations in the mixture, in Italy the Ministerial Decree of June 3rd, 2022, as an update to the decree of May 18th, 2018 mentioned in 5.1, stipulates that the concentration of hydrogen in the mixture should not exceed 2% [55].

When it comes to gas flow considerations, it is intriguing to focus on how hydrogen in the network redistributes and accumulates following separations and nodal reinjections. In chapter 4, the three scenarios involving hydrogen extraction displayed molar fractions of hydrogen across all network nodes, with varying concentrations highlighted through color gradients.

As previously emphasized, hydrogen tends to accumulate in the eastern region of the map, a result plausible given the gas flow direction and, consequently, the hydrogen mixed within it.

An interesting observation is that, despite the primary area of interest being the Syracuse Petrochemical Pole, the region exhibiting the highest accumulation percentages of hydrogen is the northeast part of the network.

This unexpected finding, initially surprising, stems from the assumption of a gas flow originating from the National network, i.e., the northern part of the map, directed towards the south.

Contrarily, as depicted in Figure 4.4, it appears that some flows were initially assumed in the wrong direction. In this case, gas seems to flow from the South towards the National network. This implies that, in addition to the initial percentages of hydrogen in the gas, this part of the network carries a substantial amount of accumulated, yet unextracted hydrogen upstream in the pipelines.

Another crucial factor is the demand for gas in the terminal nodes. As illustrated in Figure 4.2, gas demands are higher in the eastern zone compared to other areas on the map. Specifically, within this region, there is a consumption node, shown

in figure 5.4, subjected to deblending, demonstrating significantly greater demand than others. Subsequently, a high demand implies the need for a significant amount of gas to be separated, consequently leading to a high concentration of separated and reinjected hydrogen. This hydrogen must then navigate through a network segment where pipeline flow rates are lower, given the correspondingly lower final consumptions.

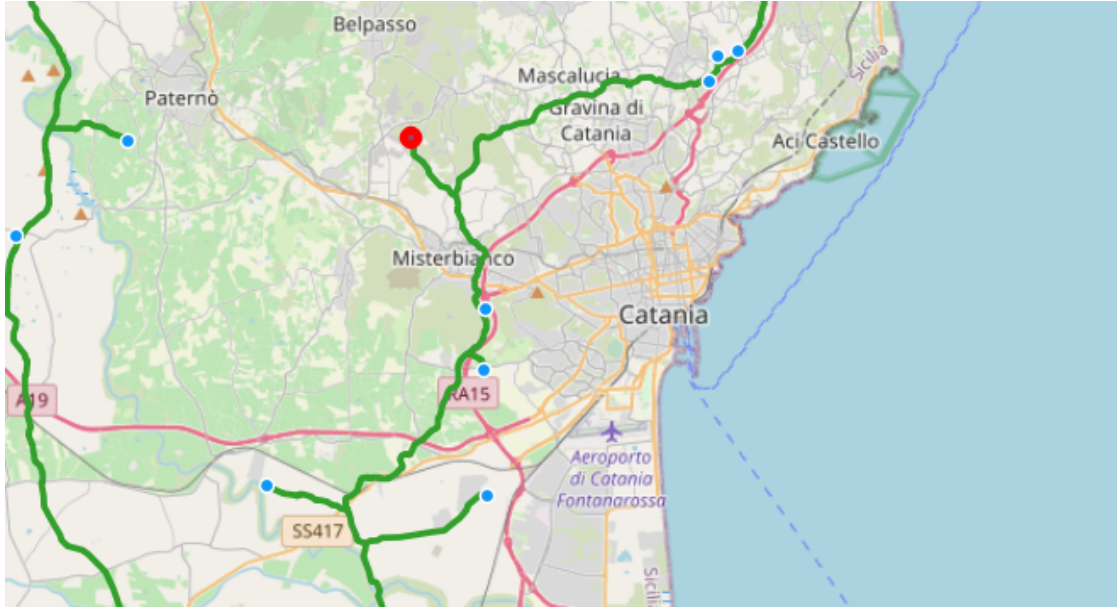


**Figure 5.4:** Geographic location of the high demand node in the area

The disparity in consumptions, coupled with the directional flow of gas, leads to an accumulation of  $H_2$  in terms of concentration.

Table 5.6 shows the flow of hydrogen in the pipeline connecting the area with the highest hydrogen concentration to the southeast area of the network, in the vicinity of the node illustrated in 5.4.

Scenario	% $H_2$	$G_{mixture}$ [kg/s]	$H_2$ [kg/s]	$H_2$ [kg/h]
5% no extr.	7.28	5.25	0.383	1377
5%	5.68	5.28	0.300	1079
10%	11.3	5.25	0.594	2138
20%	22.2	5.21	1.16	4165

**Table 5.6:** Hydrogen flow on focus pipeline

Furthermore, when considering hydrogen extraction at the refinery hub, it is

important to keep in mind that the separation yield is not flawless, and hydrogen remains in a certain percentage within the methane stream exiting for consumption. In the deblending nodes, methane percentages may vary up to 98%, while in the injection nodes, the percentages align with the established yields and purities characteristic of the deblending units chosen. With that said, hydrogen presence toward users requesting methane can be justified, although and it may occur that this percentage exceeds the 2% limit imposed by Ministerial Decree [55].

In particular, considering the worst case for this discussion, meaning 20%  $H_2$  blending, the percentage mentioned above reaches values up to 2.8%.

Finally, linking back to the amount of hydrogen extracted from the network in the petrochemical pole area, the table 5.7 summarizes the total flows as the sum of flows from all extraction nodes.

Extracted $H_2$ [kg/h]	% $H_2$ scenario
186.7	5 %
391.1	10 %
864.0	20 %

**Table 5.7:** Total  $H_2$  extraction in the three scenarios

By comparing these values with the hydrogen utilization in the Sonatrach refinery in Augusta, which has a crude oil processing capacity of 206,000 barrels per day [56], requiring approximately 3400 kg/h of hydrogen, it becomes evident that even under the highest blending scenario, the demand cannot be fully met by the hydrogen extracted from the network. Nevertheless, it could cover the 25%, the 11% and the 5.5% of the demand for a gas mixture with a 20%, 10% and 5% blend, respectively.

In 2022, Sasol Italy and Sonatrach Raffineria Italiana presented the Hybla Project which envisions the conversion of industrial areas that are no longer used, creating actual green hydrogen production and distribution centers [57]. This initiative aims to produce approximately 890 kg/h of hydrogen. For comparison, the hydrogen obtained through extraction after accumulation in our network would represent, in the three scenarios, 97%, 44% and 21% of the hydrogen produced by the Hybla Project.

However, the objective is not to completely cover the demands, but rather to quantify the amount of  $H_2$  that could be delivered by taking advantage of this form of transportation of hydrogen blended within the natural gas in order to take advantage of an already existent infrastructure without the need to completely refurbish it for the transport of 100% hydrogen or building a new infrastructure.

## **5.2 Future developments**

This thesis, given its outlined objectives, serves as a possible foundation for subsequent studies, considering the significance of the topic at both European and global levels.

A potential future investigation involves the completion and expansion of the network examined in this work, potentially encompassing the entire Sicilian region and extending to a National scale. Such an approach would allow a more comprehensive understanding of network dynamics by taking into account any inherent complexities.

The incorporation of gas from the national entry point in Mazara del Vallo could enrich the analysis by considering gases with varying qualities.

An intriguing prospect is the involvement of the Transmission System Operator of the network, facilitating the relaxation of certain assumptions through enhanced data availability. Exploring reduction facilities between the National and Regional networks could enable a more accurate reproduction of pressure drops along the network.

Additionally, having access to precise information on the location of redelivery points, perhaps through official cartography, would allow for a more accurate allocation of flow rates and more reliable results.

Finally, another option for future development could be a techno-economic analysis, factoring in the costs associated with implementing debinding technology. A techno-economic comparison with other hydrogen transportation modalities could provide a comprehensive overview, not only of the most efficient technology but also the most cost-effective one.

## 5.3 Conclusions

This thesis presents a comprehensive investigation into hydrogen deblanding within the natural gas transmission network, with a specific focus on the Southern Sicily region.

The study explores the behavior of a gas mixture originating from North Africa, comprising natural gas and green hydrogen at concentrations of 5%, 10%, and 20%. Employing data from the National Transmission System Operator and GIS tools, coupled with MATLAB simulations, the research provides insights into the integration of hydrogen into existing infrastructure.

The research aligns with the broader energy transition, recognizing hydrogen as a pivotal element in achieving carbon neutrality such as European Commission's ambitious target of a carbon-neutral continent by 2050, underscoring the urgency of sustainable energy solutions.

The methodology section transparently outlines the strategic decisions and technical processes, detailing the modeling of the gas network and the fluid dynamic simulation using the SIMPLE algorithm. However, the true significance of this work lies in the results obtained, while the simulations offer a detailed examination of gas mixture dynamics, emphasizing the deblanding process at final nodes and the gradual reintroduction of separated hydrogen into the network. Key parameters such as relative density, higher heating value, and Wobbe index are analyzed to ensure compliance with National standards.

The discussion of results unveils noteworthy patterns in hydrogen accumulation, redistribution, and demand dynamics. The relative density emerges as a crucial limiting factor as, with the minimum acceptable values observed, a 20% hydrogen concentration proves non-compliant with current directives, contrasting with acceptable 5% and 10% blends.

Further analysis reveals that even concerning higher heating value and Wobbe index intervals, a 20% hydrogen concentration falls again below the threshold value.

The observation of hydrogen redistribution and accumulation in the network following separations and nodal reinjections sheds light on gas flow considerations. Despite the primary focus on the Syracuse Petrochemical Pole, the northeast region exhibits unexpected high hydrogen accumulation percentages, challenging initial assumptions.

Addressing the demand for gas in terminal nodes, particularly in the eastern zone, emphasizes the impact of significant gas separation, leading to high concentrations of separated and reinjected hydrogen. The concluding comparison of extracted hydrogen flows with refinery usage highlights the challenges in fully meeting demand, despite covering a substantial portion.

# Bibliography

- [1] Gas Infrastructure Europe. «GIE Position on Blending Hydrogen into Existing Gas Infrastructure». In: Nov. 2021. URL: [https://www.gie.eu/wp-content/uploads/filr/5592/GIE\\_Position\\_Paper\\_on\\_Hydrogen\\_Blending.pdf](https://www.gie.eu/wp-content/uploads/filr/5592/GIE_Position_Paper_on_Hydrogen_Blending.pdf) (cit. on p. 1).
- [2] C. Fetting. *The European Green Deal*. ESDN Report. ESDN Office, 2020 (cit. on p. 2).
- [3] *Communication From The Commission To The European Parliament, The European Council, The Council, The European Economic And Social Committee And The Committee Of The Regions, The European Green Deal*. Tech. rep. COM(2019) 640 final. Brussels: European Commission, Dec. 2019 (cit. on pp. 2, 3, 5).
- [4] *Green Deal: key to a climate-neutral and sustainable EU*. European Parliament. May 2023. URL: <https://www.europarl.europa.eu/news/en/headlines/society/20200618ST081513/green-deal-key-to-a-climate-neutral-and-sustainable-eu> (cit. on p. 2).
- [5] Commissione europea and Direzione generale per l’Azione per il clima. *Going climate-neutral by 2050 : a strategic long-term vision for a prosperous, modern, competitive and climate-neutral EU economy*. Ufficio delle pubblicazioni, 2019. DOI: doi/10.2834/02074 (cit. on p. 3).
- [6] *Hydrogen roadmap Europe – A sustainable pathway for the European energy transition*. Publications Office, 2016. DOI: doi/10.2843/341510 (cit. on pp. 4, 6).
- [7] J. et al. Moja. *Hydrogen use in EU decarbonisation scenarios*. News article. European Commission, 2019 (cit. on p. 4).
- [8] *Communication From The Commission To The European Parliament, The European Council, The Council, The European Economic And Social Committee And The Committee Of The Regions, Europe’s moment: Repair and Prepare for the Next Generation*. Tech. rep. COM(2020) 456 final. Brussels: European Commission, May 2020 (cit. on p. 5).

- 
- [9] *Communication From The Commission To The European Parliament, The European Council, The Council, The European Economic And Social Committee And The Committee Of The Regions, A New Industrial Strategy for Europe*. Tech. rep. COM(2020) 102 final. Brussels: European Commission, Mar. 2020 (cit. on p. 5).
- [10] *Communication From The Commission To The European Parliament, The European Council, The Council, The European Economic And Social Committee And The Committee Of The Regions, A hydrogen strategy for a climate-neutral Europe*. Tech. rep. COM(2020) 301 final. Brussels: European Commission, July 2020 (cit. on pp. 5, 6).
- [11] *Communication From The Commission To The European Parliament, The European Council, The Council, The European Economic And Social Committee And The Committee Of The Regions, Powering a climate-neutral economy: An EU Strategy for Energy System Integration*. Tech. rep. COM(2020) 299 final. Brussels: European Commission, July 2020 (cit. on p. 5).
- [12] Ad van Wijk. *Hydrogen - a carbon-free energy carrier and commodity*. Tech. rep. Hydrogen Europe, 2021 (cit. on pp. 6, 7, 9, 10).
- [13] Tetyana Raksha, Ulrich Büniger, Uwe Albrecht, Jan Michalski, and Jan Zerhusen. *INTERNATIONAL HYDROGEN STRATEGIES A study commissioned by and in cooperation with the World Energy Council Germany*. 2020 (cit. on p. 7).
- [14] Ad van Wijk. «Hydrogen key to a carbon-free energy system». In: *Volume 3 Utilization of Hydrogen for Sustainable Energy and Fuels*. Ed. by Marcel Van de Voorde. Berlin, Boston: De Gruyter, 2021, pp. 43–104. ISBN: 9783110596274. DOI: [doi:10.1515/9783110596274-005](https://doi.org/10.1515/9783110596274-005). URL: <https://doi.org/10.1515/9783110596274-005> (cit. on p. 8).
- [15] *The Future of Hydrogen*. Tech. rep. License: CC BY 4.0. Paris: IEA, June 2019 (cit. on p. 9).
- [16] McKinsey. *Hydrogen Insights, A perspective on hydrogen investment, market development and cost competitiveness*. Tech. rep. HydrogenCouncil, Feb. 2020 (cit. on pp. 10, 11).
- [17] Ad van Wijk. «Hydrogen key to a carbon-free energy system». In: *Volume 1, Hydrogen Production and Energy Transition*. Ed. by Marcel Van de Voorde. Berlin, Boston: De Gruyter, 2021, pp. 43–104. DOI: <https://doi.org/10.1515/9783110596250-005>. URL: <https://doi.org/10.1515/9783110596250-005> (cit. on p. 10).
- [18] *How to transport and store hydrogen? Facts and figures*. Tech. rep. ENTSOG, GIE and Hydrogen Europe, May 2021 (cit. on pp. 12, 20, 22, 23).

- [19] *Response to EC Public Consultation: Strategy for Energy System Integration*. Tech. rep. Hydrogen Europe, Mar. 2022 (cit. on pp. 12, 13).
- [20] *How a dedicated hydrogen infrastructure can be created*. Tech. rep. European Hydrogen Backbone, 2020 (cit. on pp. 13, 23).
- [21] *Hydrogen infrastructure – the pillar of energy transition – The practical conversion of long-distance gas network to hydrogen operation*. Tech. rep. Nowega: Siemens Energy, 2020 (cit. on pp. 15, 20, 22).
- [22] *The European Hydrogen Backbone (EHB) initiative*. European Hydrogen Backbone. 2023. URL: <https://ehb.eu/#:~:text=Participating%20companies%20include%20Amber%20Grid,%2C%20Nordion%20Energi%2C%20OGE%2C%20ONTRAS> (cit. on pp. 16, 18).
- [23] *Proposal for a Directive of the European Parliament and of the Council on common rules for the internal markets in renewable and natural gases and in hydrogen*. Tech. rep. COM(2021) 803 final. Brussels: European Commission, Dec. 2021 (cit. on p. 16).
- [24] *Proposal for a Regulation of the European Parliament and of the Council on the internal markets for renewable and natural gases and for hydrogen (recast)*. Tech. rep. COM(2021) 804 final. Brussels: European Commission, Dec. 2021 (cit. on p. 16).
- [25] *Communication From The Commission To The European Parliament, The European Council, The Council, The European Economic And Social Committee And The Committee Of The Regions, Powering a climate-neutral economy. REPowerEU: Joint European Action for more affordable, secure and sustainable energy*. Tech. rep. COM(2022) 108 final. Strasbourg: European Commission, Mar. 2022 (cit. on p. 16).
- [26] *A European Hydrogen Infrastructure Vision Covering 28 Countries*. Tech. rep. European Hydrogen Backbone, 2022 (cit. on pp. 16, 17, 19, 35, 36).
- [27] *Analysing future demand, supply, and transport of hydrogen*. Tech. rep. European Hydrogen Backbone, 2021 (cit. on p. 17).
- [28] Carbon Limits and DNV. *Study on the reuse of oil and gas infrastructure for H2 and CCS in Europe*. Tech. rep. Re-Stream, 2021 (cit. on p. 20).
- [29] *Extending the European Hydrogen Backbone*. Tech. rep. Gas for Climate, Guidehouse, 2021 (cit. on p. 20).
- [30] *Decarbonising the gas value chain. Challenges, solutions and recommendations*. Tech. rep. ENTSOG, 2021 (cit. on pp. 21, 22, 24, 25).
- [31] *A Renovation Wave for Europe - greening our buildings, creating jobs, improving lives*. Tech. rep. COM(2020) 662 final. Brussels: European Commission, 2020 (cit. on p. 21).

- [32] *COUNCIL DIRECTIVE 93/68/EEC*. Tech. rep. Brussels: Official Journal of the European Communities, 1993 (cit. on p. 21).
- [33] et al. B. von Manteuffel. *EU pathways to a decarbonised building sector*. Tech. rep. Ecofys, 2016 (cit. on p. 21).
- [34] *A flexible approach for handling different and varying gas qualities*. Tech. rep. ENTSOG, 2018 (cit. on p. 24).
- [35] *First ACER Implementation Monitoring Report of the Network Code on Interoperability and data exchange*. Tech. rep. ACER, 2017 (cit. on p. 24).
- [36] Kun Tan, Devinder Mahajan, and T.A. Venkatesh. «Computational fluid dynamic modeling of methane-hydrogen mixture transportation in pipelines: Understanding the effects of pipe roughness, pipe diameter and pipe bends». In: *International Journal of Hydrogen Energy* (2023). ISSN: 0360-3199. DOI: <https://doi.org/10.1016/j.ijhydene.2023.06.195>. URL: <https://www.sciencedirect.com/science/article/pii/S0360319923031488> (cit. on pp. 25, 27).
- [37] Xiao Tian and Jingjing Pei. «Study progress on the pipeline transportation safety of hydrogen-blended natural gas». In: *Heliyon* 9.11 (2023). ISSN: 2405-8440. DOI: <https://doi.org/10.1016/j.heliyon.2023.e21454>. URL: <https://www.sciencedirect.com/science/article/pii/S2405844023086620> (cit. on pp. 25–27).
- [38] Li Yuxing, Zhang Rui, Liu Cuiwei, et al. «Hydrogen embrittlement behavior of typical hydrogen-blended natural gas pipeline steel». In: *Oil & Gas Storage and Transportation* 41.6 (2022), pp. 732–742 (cit. on p. 26).
- [39] Yan Zhao, Vincent McDonell, and Scott Samuelsen. «Experimental assessment of the combustion performance of an oven burner operated on pipeline natural gas mixed with hydrogen». In: *International Journal of Hydrogen Energy* 44.47 (2019), pp. 26049–26062. ISSN: 0360-3199. DOI: <https://doi.org/10.1016/j.ijhydene.2019.08.011>. URL: <https://www.sciencedirect.com/science/article/pii/S0360319919329258> (cit. on p. 27).
- [40] Irfan Ahmad Gondal. «Hydrogen integration in power-to-gas networks». In: *International Journal of Hydrogen Energy* 44.3 (2019), pp. 1803–1815. ISSN: 0360-3199. DOI: <https://doi.org/10.1016/j.ijhydene.2018.11.164>. URL: <https://www.sciencedirect.com/science/article/pii/S0360319918337960> (cit. on p. 27).
- [41] *Hydrogen Deblending in the GB Gas Network*. NIA Final Report. National Grid, 2021 (cit. on pp. 28–33).

- [42] Carlos A. Grande. «Advances in Pressure Swing Adsorption for Gas Separation». In: *International Scholarly Research Notices* 2012. Article ID 982934 (20112), p. 13. DOI: <https://doi.org/10.5402/2012/982934> (cit. on p. 30).
- [43] *Hydrogen Recovery by Pressure Swing Adsorption*. Tech. rep. Linde (cit. on p. 30).
- [44] Martuzzi M. Mudu P. Terracini B. *Human Health in Areas with Industrial Contamination*. World Health Organization, 2014 (cit. on p. 36).
- [45] *Rete Snam rete gas e infrastrutture trasporto gas*. Snam. May 2023. URL: <https://www.snam.it/it/i-nostri-business/trasporto/servizi-online/la-rete/rete-gas-e-infrastrutture-trasporto-gas.html> (cit. on p. 38).
- [46] *Caratteristiche tecniche della rete*. Snam. 2023. URL: <https://www.snam.it/it/i-nostri-business/trasporto/servizi-online/la-rete/caratteristiche-tecniche-della-rete.html> (cit. on p. 39).
- [47] *Capacità di trasporto punti di riconsegna*. Snam. May 2023. URL: [https://www.snam.it/it/trasporto/Processi\\_Online/Capacita/informazioni/capacita-trasporto/Capacita\\_trasporto/02\\_PdR/02a/02a\\_Elenco.html](https://www.snam.it/it/trasporto/Processi_Online/Capacita/informazioni/capacita-trasporto/Capacita_trasporto/02_PdR/02a/02a_Elenco.html) (cit. on p. 43).
- [48] *Capacità di trasporto punti di entrata e di uscita di rete nazionale*. Snam. May 2023. URL: [https://www.snam.it/it/trasporto/Processi\\_Online/Capacita/informazioni/capacita-trasporto/Capacita\\_trasporto/01\\_Entrata\\_uscita/01a/01a\\_Elenco.html](https://www.snam.it/it/trasporto/Processi_Online/Capacita/informazioni/capacita-trasporto/Capacita_trasporto/01_Entrata_uscita/01a/01a_Elenco.html) (cit. on p. 43).
- [49] *PCS convenzionale*. Snam. 2023. URL: [https://www.snam.it/it/trasporto/adempimenti-reporting-autorita/PCS\\_Convenzionale/](https://www.snam.it/it/trasporto/adempimenti-reporting-autorita/PCS_Convenzionale/) (cit. on p. 44).
- [50] M. Cavana. «Gas network modelling for a multi-gas system». Doctoral Dissertation: Doctoral Program in Energetics. ScuDo - Politecnico di Torino, 2020 (cit. on p. 45).
- [51] G. Nosedà D. Citrini. *Idraulica*. Casa editrice Ambrosiana, 1987 (cit. on p. 48).
- [52] Ministero dello Sviluppo Economico. «Aggiornamento della regola tecnica sulle caratteristiche chimico-fisiche e sulla presenza di altri componenti nel gas combustibile da convogliare». In: (May 2018). DOI: [GUSerieGeneralen.129](https://doi.org/10.1080/11257454.2018.1481129) (cit. on pp. 67, 68).
- [53] *Gas Tipici*. Snam Rete Gas. 2022. URL: <https://misura.snam.it/portmis/coortecDocumentoController.do?menuSelected=4300> (cit. on p. 68).
- [54] *Fuels - Higher and Lower Calorific Values*. The Engineering ToolBox. 2003. URL: [https://www.engineeringtoolbox.com/fuels-higher-calorific-values-d\\_169.html](https://www.engineeringtoolbox.com/fuels-higher-calorific-values-d_169.html) (cit. on p. 68).

## BIBLIOGRAPHY

---

- [55] Ministero dello Sviluppo Economico. «Aggiornamento al decreto del Ministro dello sviluppo economico 18 maggio 2018». In: (June 2022). DOI: [GUSerieGeneralen.139](https://doi.org/10.2430/1139) (cit. on pp. 71, 73).
- [56] *Sustainability report 2022*. Tech. rep. Sonatrach Raffineria Italiana S.r.l., 2022 (cit. on p. 73).
- [57] *Progetto Hybla: Sasol e Sonatrach per la produzione di idrogeno e syngas low carbon con cattura di CO<sub>2</sub>*. Energia e Mercato. 2023. URL: <https://www.energiamercato.it/notizie/sistema-italia/progetto-hybla> (cit. on p. 73).